3.03
Continental Basaltic Rocks

G. L. Farmer

University of Colorado, Boulder, CO, USA

3.03.1 INTRODUCTION

During the past few decades, geochemical studies of continental basaltic rocks and their petrologic kin have become mainstays of studies of the continental lithosphere. These igneous rocks have taken on such an important role largely because the chemical and isotopic composition of continental basaltic rocks and their mantle (see Chapter 2.05) and crustal xenoliths (see Chapter 3.01) provide the best proxy record available to Earth scientists for the chemical and physical evolution of the deep continental lithosphere and underlying mantle, areas that are otherwise resistant to direct study. Keeping this in mind, the primary goal of this chapter is to illustrate how geochemical data can be used both to assess the origin of these rocks and to study the evolution of the continental lithosphere.

A complete overview of continental basaltic rocks will not be attempted here, because continental "basalts" come in too wide a range of compositions, and because of the sheer volume of geochemical data available for such rocks worldwide. The scope of the chapter is limited to a discussion of a select group of ultramafic to mafic composition "intraplate" continental igneous rocks consisting primarily of kimberlites, potassic and sodic alkali basalts, and continental flood basalts (CFBs). Igneous rocks forming at active continental margins, such as convergent or transform plate margins, are important examples of continental magmatism but are not directly discussed here (convergent margin magmas are discussed in Chapters 2.11, 3.11, and 3.18). The geochemistry of intraplate igneous rocks of the ocean basins is covered in Chapters 2.04 and 3.16. Although basaltic magmatism has occurred throughout the

Earth's history, the majority of the examples presented here are from Mesozoic and Cenozoic volcanic fields due to the more complete preservation of younger continental mafic igneous rocks. While considerable effort has been expended in studying the chemical differentiation of mafic magmas, the present discussion concentrates on the least differentiated basaltic rocks in a given location. Such rocks generally provide the best estimate of the compositions of "primary" magmas generated beneath a given volcanic field, and primary magmas provide the most direct insights into the nature of the magma source regions.

3.03.2 GENERAL PRINCIPLES

Intraplate continental ultramafic to mafic magmatism ranges in volume from $<5\,km^3$ of erupted material for kimberlite pipes and alkali basalt volcanic centers to $>2{,}500\,km^3$ for individual CFB flows associated with "large igneous provinces (LIPs)" (Sigurdsson, 2000). Regardless of the volume involved, petrologists are faced with similar questions when attempting to define the origin of any continental igneous rock: where, and why, did the melting occur that ultimately led to the formation of that rock? This information is not simple to extract from the composition of a given igneous rock, because its composition is influenced both by the composition of the magmatic source region—which, in the case of the continental lithosphere, can be highly heterogeneous—and through the processes by which the magma was generated and then modified during transport to shallower depths in the lithosphere. Nevertheless, because mafic continental igneous rocks could have been derived from or have extensively interacted with the continental lithosphere, they contain information regarding the chemical and isotopic composition and the physical state of the deep lithosphere.

Although defining the origin and evolution of mafic continental magmatism is a complex task, there are certain basic tenets regarding the possible source regions of such magmas and the factors influencing magma chemical and isotopic compositions that can be used to help constrain the origin of a given igneous rock. These tenets are outlined in the following sections.

3.03.2.1 Potential Sources of Continental Mafic Magmatism

It is generally conceded that ultramafic to mafic magmas are the products of partial melting of ultramafic rocks in the Earth's upper mantle (Kushiro, 2001; see Chapter 2.08). The composition of primary magmas generated by partial melting of ultramafic mantle rocks are, in turn, controlled by the mineralogy and chemical composition of the ultramafic rocks, as well as by the pressure, temperature, and extent of partial melting (Grove, 2000). A "primary" magma, for our purposes, is a magma produced at depth in the Earth, the composition of which is controlled by the mineralogic and chemical makeup of the source and the conditions of melting, and has not been modified by differentiation during ascent to shallower depths (Winter, 2001). Basalts representing primary magmas derived from the melting of the upper mantle are simple to recognize, if not commonly found, because magmas that were in equilibrium with magnesium-rich olivine ($mg\# = Mg/(Mg + Fe^{2+}) = 0.90$) in the mantle will also have high mg# (~ 0.73; Grove, 2000).

The ability of the mantle to produce basaltic magmas, generally referred to as its "fertility," is a fundamental parameter controlling where primary continental basaltic rocks can be generated. For a typical lherzolitic mantle, consisting of olivine, orthopyroxene, clinopyroxene, and an aluminous phase (either plagioclase, spinel, or garnet, depending on depth), extraction of a basaltic magma results in a decrease in whole-rock aluminum, silicon, iron, sodium, calcium, titanium, and chromium contents, and a relative increase in magnesium concentrations (and an increase in the whole-rock mg#; Frey and Green, 1974; Griffin *et al.*, 1999). Mineralogically, basaltic magma production from lherzolite generally consumes clinopyroxene, resulting in a mantle residuum of either harzburgite (olivine + orthopyroxene) or even dunite (i.e., olivine) when the percentage of partial melting is high (Winter, 2001). As a result, continental basalts must either be produced from portions of the mantle that have remained fertile for basalt generation throughout Earth history, or that have been subsequently refertilized with basaltic components through metasomatism by infiltrating fluids and/or magmas (Kelemen *et al.*, 1998; Griffin *et al.*, 1999).

Where are the potential fertile mantle sources for continental basalt generation? In simplest terms, two possibilities exist: the continental lithospheric mantle (CLM) and the underlying upper mantle. The latter is sometimes referred to as the "asthenosphere" by geochemists (Figure 1). Unfortunately, the definitions of lithosphere and asthenosphere used for geochemical purposes have been the source of some confusion (Anderson, 1995). Here, the definition of continental "lithosphere" is adopted (White, 1988), in which the lithosphere

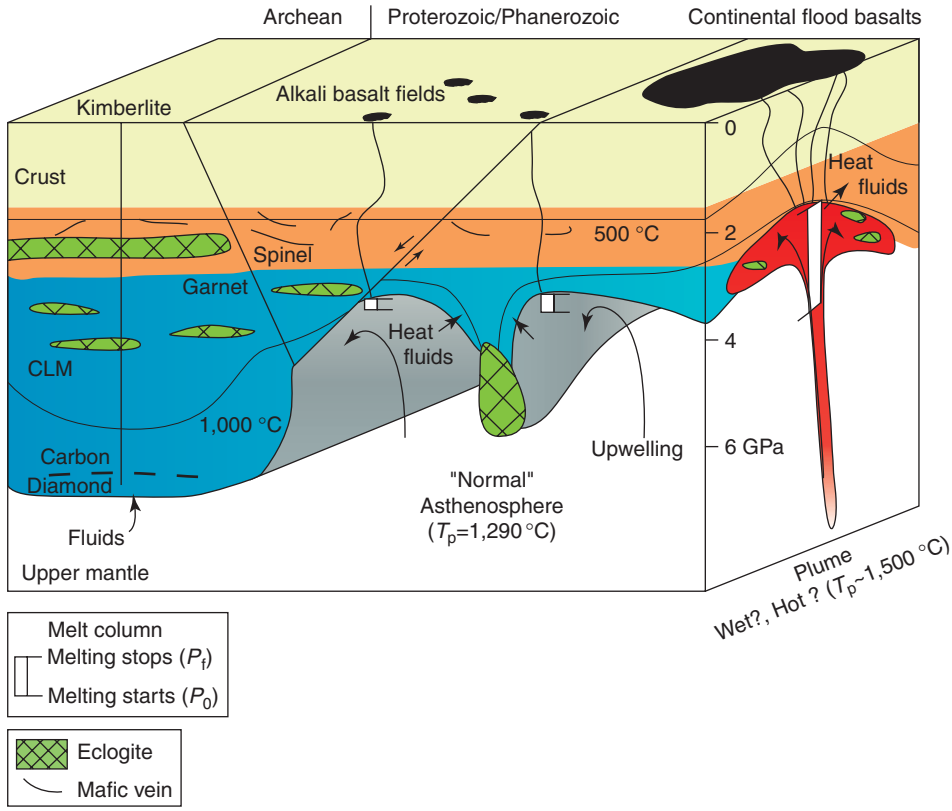

Figure 1 Cartoon depicting continental crust and mantle lithosphere (CLM), underlying sublithospheric mantle, and potential sources of ultramafic to mafic composition continental magmatism.

is considered to be the "outer shell of the Earth where there is a conductive temperature gradient, overlying the well-mixed adiabatic interior." In this definition, the adiabatic "interior" includes the convecting, sublithospheric, upper mantle, embedded in which is the shallow, weak, and presumably partially molten asthenosphere.

The above definition of the lithosphere equates the lithosphere with a thermal boundary layer (TBL), a layer in which heat is transferred by conduction and not by advection (Anderson, 1995). As a result, the base of the lithosphere by this definition essentially represents the depth at which the conductive geotherm of the lithosphere intersects the adiabat describing temperature as a function of depth in the underlying convecting mantle (Rudnick *et al.*, 1998). Note that the lithosphere, as originally defined on the basis of its high viscosity and high strength (Barrell, 1914), represents at best only the upper half of the TBL (Anderson, 1995). Therefore, the base of the lithosphere, as defined here, is not necessarily strong and permanent. In fact, some workers have argued that the base of the lithosphere, if hydrated, becomes weak and subject to flow (Anderson, 1995).

The sublithospheric mantle is involved in the production of voluminous basaltic magmatism at mid-ocean ridges (see Chapter 3.13), and so is obviously fertile for basalt production. In contrast, the fertility of the continental mantle lithosphere is more variable. The continental mantle lithosphere, unlike its oceanic counterpart, may not have been isolated from the convecting portions of the mantle solely through progressive conductive cooling through time. It has long been argued that the mantle portions of the Archean continental lithosphere may be compositionally distinct from the mantle lithosphere associated with younger crustal segments or oceanic lithosphere due to the extraction of large melt fractions from the upper mantle during Archean crust formation (Jordan, 1978, 1988). Komatiites, which are primarily Archean, highly magnesian (>18 wt.% MgO; Le Bas, 2000) extrusive igneous rocks, likely represent the products of such large degrees of mantle melting (either in anhydrous, hot plume, or wet Archean subduction zones; Arndt *et al.*, 1998; Parman *et al.*, 2001). Extraction of komatiitic magma increases the buoyancy of the mantle due to the preferential removal of iron (relative to magnesium) into the magma. The resulting decrease

in the density of the residual mantle could account both for the preferential preservation of the Archean mantle and the great thickness (>200 km; Figure 1) proposed for many Archean cratons (Jordan, 1988). However, thick, unmetasomatized Archean mantle lithosphere is also likely to be refractory, and therefore infertile when it comes to the production of basaltic magmas. In contrast, post-Archean CLM could be sufficiently fertile (Jordan, 1988) to spawn additional basaltic magmatism. It should also be noted that variations in CLM compositions affect lithospheric strength (Lee *et al.*, 2001), and as a result the fertile mantle lithosphere may be more susceptible to thinning, either through stretching or the development of lithospheric mantle "drips" (Figure 1).

Although ultramafic lithologies in the CLM and underlying mantle are the principal sources of continental basaltic magmas, both the lithospheric and sublithospheric mantles are heterogeneous and can contain mafic lithologies that might become involved in magma production. For example, pyroxenites, websterites, eclogites, etc. exist as veins and/or discrete layers in portions of the continental mantle (Wilshire *et al.*, 1991; see also Chapters 2.04 and 2.05). Although these lithologies are generally thought to produce intermediate to silicic, and not mafic, magmas when partially melted (Leeman and Harry, 1993; see Pertermann and Hirschmann (2003) for an alternative view), magmatic contributions by mafic lithologies can influence both the composition and the volume of mafic magmas produced in the upper mantle (Cordery *et al.*, 1997).

3.03.2.2 Trigger Mechanisms for Mantle Melting

Mantle melting simply requires that the mantle temperature, at a given pressure, exceeds its solidus temperature. This can be induced in the mantle either by heating, decompression, or a change in chemical composition, particularly the addition of volatiles, which greatly reduces the mantle solidus temperature (see also Chapter 2.07; Figure 2). Each of these

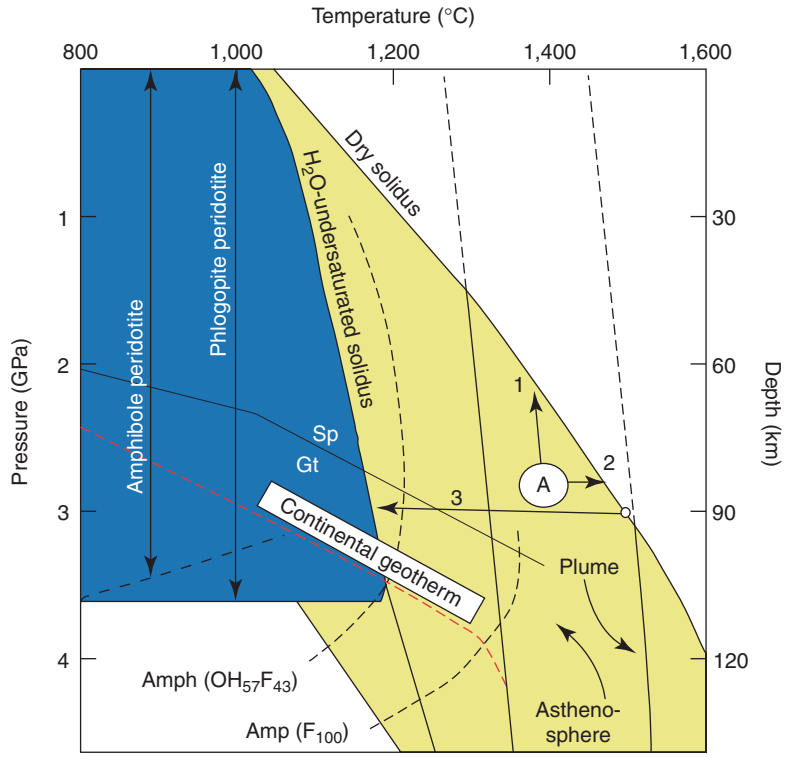

Figure 2 Pressure versus temperature plot for the upper mantle, showing both dry and H_2O undersaturated solidi for lherzolite. Melting of dry mantle originally at point "A" can be induced either by adiabatic upwelling (path "1"), conductive heating (path "2"), or addition of volatiles, which lowers the mantle solidus temperature (path "3"). The diagram also illustrates that amphibole and phlogopite are unlikely to be present in either normal asthenosphere, or hot mantle plumes because these phases break down at higher temperatures. Both phases are apparently stable only in colder lithospheric mantle. Fine dashed lines show stability limits of amphiboles with various fluorine contents. Shaded area is stability range of phlogopite. Sp = spinel, Gt = garnet. After Class and Goldstein (1997) and le Roex *et al.* (2001).

processes can be relevant in the formation of continental magmatism. For example, consider melting in the sublithospheric mantle. Decompression melting of this mantle can be induced by lithospheric thinning associated with continental extension, particularly during the formation of continental rifts (Figure 1). Melting occurs when the deeper mantle flows upwards to compensate for the decreased lithospheric thickness. In a seminal paper, McKenzie and Bickle (1988) numerically modeled this process and demonstrated that the higher the sublithospheric mantle-potential temperature (T_p, the temperature that the mantle would have should it be allowed to rise adiabatically to the Earth's surface) and the greater the degree of lithospheric extension, the larger the depth interval in the mantle over which melting occurs (the polybaric "melt column," Figure 1) and, consequently, the larger the volume of melt produced. In general, the thicker the continental lithosphere and the colder the sublithospheric mantle, the smaller the volume of magma produced by sublithospheric mantle melting. For example, decompression melting of "normal" potential temperature (1,290 °C) sublithospheric mantle induced by lithospheric extension may occur through only a short pressure interval because the melt column is effectively capped by the base of the CLM (Figure 1). As a result, only small melt volumes are generated, as observed in alkali basalt volcanic fields (Figure 1) and melting may be restricted to the garnet peridotite stability field. Conversely, the hotter the sublithospheric mantle, the greater the depth of initiation of melting and the volume of magma produced in upwelling mantle, even in the absence of thinning lithosphere; hence, the likely importance of high-potential temperature mantle plumes in the generation of large-volume CFBs (Figure 1). Decompression melting in the sublithospheric mantle can also be induced within convective instabilities in the upper mantle resulting from original variations in lithospheric thickness (King and Anderson, 1998) or lithospheric "delamination" (Elkins and Hager, 2000).

Decompression melting in the continental mantle lithosphere, in contrast, is difficult to induce, even in fertile mantle (Arndt and Christensen, 1992). Harry and Leeman (1995), for example, demonstrated that lithospheric extension does not typically bring either dry or water-saturated peridotite into supersolidus conditions (Figure 3). Instead, melting of the lithospheric mantle seems to require the addition of fluids and/or heat from the underlying mantle (Harry and Leeman, 1995). Turner *et al.* (1996b) demonstrated that conductive heating of hydrated lithospheric mantle by an upwelling mantle plume can produce significant volumes of melt depending, in part, on the original thickness of hydrated mantle.

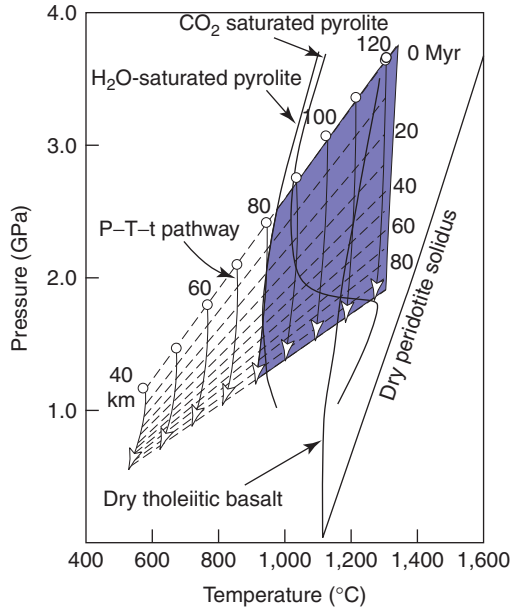

Figure 3 Pressure versus temperature plot showing calculated temperatures of lithospheric mantle as a function of time during an episode of lithospheric extension. The shaded area is mantle with pressures and temperatures above the H_2O-saturated solidus. In the example shown, the lithospheric mantle that originally ($t = 0$) spanned the depth interval from 40 to 125 km undergoes extension and thinning at a rate of 5 mm yr^{-1}. The diagram illustrates that dry peridotite mantle does not cross its solidus during ascent associated with lithospheric extension. As a result, extension cannot generally induce melting in dry, lithospheric peridotite. Similarly, hydrated, shallow (<80 km) peridotite does not cross the lower-temperature wet solidus during extension. Melting of lithospheric peridotite instead requires hydration of initially dry mantle and/or conductive heating from the underlying mantle, for example, during plume impact (Turner *et al.*, 1996b). However, melting of mafic lithologies within CLM can occur if the mantle crosses the basalt solidus during extension. Reproduced by permission of American Geophysical Union from Harry and Leeman (1995).

Clearly, then, the physical and chemical characteristics of the continental lithosphere play an important role in determining the sources and volumes of continental mafic magmatism. Therefore, if the sources of a given continental igneous rock can be determined, then inferences can be made regarding the dynamic processes in the subcontinental mantle during magma generation. The difficulty is to determine unambiguously the source

of a given continental basalt. For this purpose, the geochemist must rely on indirect information regarding magma source regions provided by a basalt's major-, trace-element, and isotopic composition.

3.03.2.3 Factors Influencing Magma Major Element Compositions

Petrologic and major-element studies of Cenozoic continental basaltic rocks have defined two primary magma "series" in intraplate basaltic igneous rocks: alkalic, and tholeiitic (the latter comprising, along with "calc-alkalic," the subalkalic series of Iddings, 1892). Alkalic continental basalts typically have lower silicon and higher sodium and potassium contents than tholeiitic basalts, while the latter show a characteristic pattern of initial iron enrichment during differentiation (Winter, 2001). A primary goal of modern studies in igneous petrology has been to determine what factors lead to the production of these two magma series, in particular, to assess the relative importance of mantle source composition and the physical parameters of melting in controlling melt composition. One line of thought is that the two magma series represent different degrees and depths of melting of dry peridotite. Experimental studies have shown that small degrees of melting ($<5\%$, by wt.) of peridotite at pressures greater than 3 GPa produces primary alkali magmas of basaltic composition, while larger degrees of melting of the same source at shallower depths can generate tholeiitic series basaltic magmas (Hirose and Kushiro, 1993; see Chapter 2.08). Other workers, however, argue that compositional variations in the mantle source are required to produce the various magma series. In particular, the generation of highly potassic alkaline magmas has been attributed to melting within ultramafic mantle containing metasomatically introduced, potassium-rich, hydrous mineral phases such as phlogopite or potassic amphibole (e.g., K-richterite; Foley, 1992). The metasomatic addition of alkali elements and volatile constituents, principally CO_2 or H_2O, to the lithospheric mantle via fluids and/or melts from the sublithospheric mantle is key to the generation of other alkaline continental igneous rocks, including kimberlites, carbonatites, and lamproites (Wyllie and Huang, 1976; see Chapter 2.07).

Understanding the range of major-element compositions produced by polybaric decompression melting of the sublithospheric mantle has also been a focus of recent research efforts, in part because theoretical and experimental studies in the 1990s have provided a detailed picture of the compositions of primary magmas produced through melting of spinel and garnet peridotites (Baker and Stolper, 1994). Most notably, Langmuir *et al.* (1992) used information on the partitioning of magnesium and iron between olivine and magma (Roeder and Emslie, 1970), and sodium (an incompatible element) partitioning between mantle clinopyroxene and melt to model the composition of magmas as a function of the depth of melt initiation and the extent of melting. The results of these calculations illustrate that iron contents of primary magmas derived from mantle peridotite increase with increasing depth of melt initiation, and that the sodium content decreases regularly with the extent of mantle melting (Figure 4). The sodium and iron contents of a given suite of basaltic rocks can therefore provide constraints on the physical conditions of decompression mantle melting. Several workers have attempted to use these systematics to investigate the depth of origin and the extent of mantle melting of certain continental basaltic rocks, including alkali basalts (Wang *et al.*, 2002) and CFBs (Basu *et al.*, 1998).

3.03.2.4 Factors Influencing Magma Trace-Element Abundances

The trace-element abundances in basaltic rocks can also be used to gain insights into the composition of the basalt source regions and the physical processes involved in melting and magmatic differentiation (see Rollinson, 1993), for a comprehensive review). Trace elements, which are defined as elements that are present at concentrations <0.1 wt.%, are usually not sufficiently abundant to form their own mineral phases in the mantle but substitute to varying degrees in existing mineral structures, depending largely on their ionic size and charge (see Chapter 2.09). During partial melting, the trace elements partition between the residual mineral phases and coexisting liquid. Incompatible elements partition dominantly into the liquid phase, and so have low-mineral/melt partition coefficients, D, which are functions of the physical conditions during melting and of the melt composition ($D =$ mineral/melt partition coefficient = (concentration of element, i, in mineral)/(concentration of i in coexisting melt)). Compatible elements, in contrast, have high D values and partition into the solid phase.

A simple application of these systematics in studies of basalt petrogenesis involves constructing ratios of incompatible to potentially

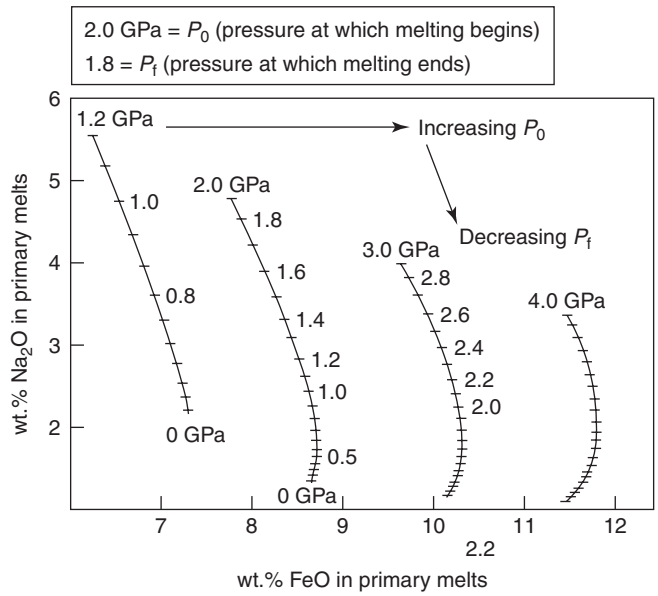

Figure 4 Plot of Na_2O versus FeO (wt.%) for products of polybaric melting of peridotitic mantle using the model of Langmuir *et al.* (1992). Each line shows a polybaric melting "path" during adiabatic decompression from the depth (pressure) where melting commenced, P_0, to a final depth of melting, P_f. The compositions of fractional melts produced during decompression melting of the mantle are accumulated and the resulting bulk compositions are plotted at intervals of 0.1 GPa (tick marks on each line; numbers in italics are values for P_f). The results of these calculations illustrate that dry peridotite of uniform composition will show increasing Fe contents as P_0 increases (essentially as potential temperature of mantle increases) while Na contents decrease with increasing extent of melting (i.e. as P_f decreases). Reproduced by permission of American Geophysical Union from Wang *et al.* (2002).

compatible (or, at least, less incompatible) elements during mantle melting. Such ratios, when corrected for modifications that may have occurred during magmatic differentiation, can provide information regarding the mineral phases that might have remained in the mantle source at the time the basaltic magmas were generated. This information can, in turn, provide information regarding the composition and depth of the mantle source. One popular ratio used for this purpose is $(La/Yb)_N$ (where N indicates that this is the ratio of lanthanum and ytterbium abundance normalized to the abundance of these elements in chondritic meteorites). Lanthanum, a light rare-earth element (LREE), is highly incompatible in minerals of spinel and garnet peridotite, while ytterbium, a heavy rare-earth element (HREE), is incompatible in spinel but not garnet (D for ytterbium in garnet is >3; Thirlwall *et al.*, 1994). As a result, a high $(La/Yb)_N$ ($> \sim 5$; Thirlwall *et al.*, 1994), or low Lu/Hf (Beard and Johnson, 1997) in primary basaltic magmas can be attributed to melting in the presence of residual garnet and therefore requires that at least some portion of the melting must have occurred at depths below the spinel to garnet transition in mantle peridotites (Figures 1 and 2). Fractionation of thorium from uranium in basaltic magmas, as manifested in the uranium-series disequilibria observed in some young continental basalts (Asmerom, 1999), may also be controlled by the presence of residual garnet, due to the greater compatibility of uranium in this mineral (Beattie, 1993), although recent experimental studies have demonstrated that clinopyroxene can also fractionate uranium from thorium, even during melting of spinel peridotite (Landwehr *et al.*, 2001).

Other elements are also uniquely partitioned into specific mantle mineral phases. For example, potassium, rubidium, and barium partition preferentially into phlogopite (Schmidt *et al.*, 1999). Relative depletions in the abundances of these elements on primitive mantle normalized trace-element plots (see later sections) can therefore serve as evidence of residual phlogopite in the source region of basaltic rocks. Amphibole can also sequester potassium and barium, as well as strontium and the middle REE (gadolinium through erbium), and both phases can incorporate titanium, niobium, and tantalum (i.e., high-field-strength elements, HFSE; Dalpé and Baker, 2000). Recognition of the trace-element signatures of residual phlogopite and amphibole in basalts

is significant, because both mineral phases are unstable at the high temperatures of the convecting upper mantle and therefore imply basalt derivation from, or interaction with, the lithospheric mantle (Figure 2; Class and Goldstein, 1997).

It is also possible to use the ratios of highly incompatible elements in basaltic rocks to determine these ratios in their mantle source regions, given that elements having similar K_d values produce incompatible element ratios that are independent of the degree of partial melting of the mantle source or the amount of subsequent magmatic differentiation (Hanson, 1989; Hofmann, 1997). The ratio of niobium to uranium has proved useful in fingerprinting ocean-island basalts (OIBs) and for distinguishing these basalts from those produced in subduction environments (island-arc basalts (IAB)). The latter (together with continental crust) have uniquely low Nb/U, as well as low Rb/Cs, and Ce/Pb ratios, relative to both OIB and mid-ocean ridge basalts (MORBs) (Figure 5; McDonough *et al.*, 1992; Hofmann, 1997). The origin of the relative depletions in niobium, tantalum, and titanium, and the enrichments in lead and the large-ion lithophile elements' (LILEs; rubidium, barium, cesium, etc.) abundances in IABs remains a matter of debate, but most likely is due to a combination of the high mobility of lead and LILE in fluids produced during the dehydration of subducting oceanic lithosphere and the sequestering of some HFSE in an Fe–Ti mineral stable in the down-going slab (Ryerson and Watson, 1987; Pearce and Peate, 1995).

The incompatible element ratios of oceanic basalts provide a convenient template against which to compare the trace-element characteristics of continental basaltic rocks. Intraplate continental basalts can also be distinguished on the basis of their Nb/U and Ce/Pb ratios, with "low-titanium" potassic alkali basalts (loosely defined as containing <2 wt.% TiO_2, Figure 6, and Ti/Y <310; Peate, 1997) having significantly lower ratios than kimberlites and "high-titanium" alkali basalts (Figure 5). This observation implies that intraplate continental basalts may be derived from mantle source regions that are chemically similar to the sources of oceanic basalts and IABs, although enthusiasm for such a straightforward conclusion must be tempered by the fact that contamination of primary mantle-derived magmas by continental crust can lower both ratios (see Section 3.03.2.6).

More elaborate modeling of the relative trace-element abundances of basaltic rocks has long been undertaken, using both forward (Shaw, 1970) and inverse techniques (McKenzie and O'Nions, 1991). These studies have demonstrated that the relative trace-element abundances of primary melts of the mantle are influenced not only by the pertinent mineral/melt partition coefficients, but also by the initial trace-element abundances of the rock, and the style and degree of melting (i.e., batch versus fractional melting, congruent versus incongruent melting; Zou and Reid, 2001). As a result, while quantitative models continue to provide important insights into the origin of continental igneous rocks (e.g., Tainton and McKenzie, 1994), their interpretation remains fraught with uncertainties due to the number of unconstrained variables involved in the calculations.

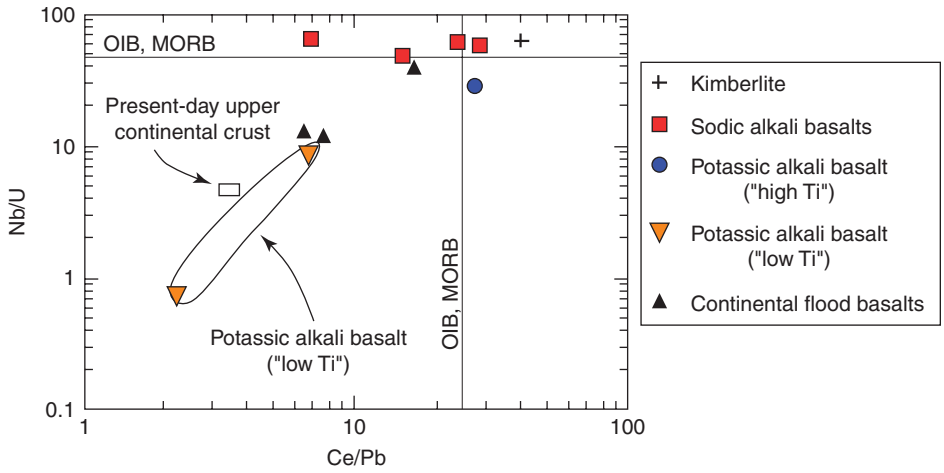

Figure 5 Average Ce/Pb and Nb/U from selected kimberlites, continental alkali basalts, and CFBs. Present-day continental crust values from Condie (1993), and MORB and OIB values from Hofmann (1997) (data from Tables 1–3).

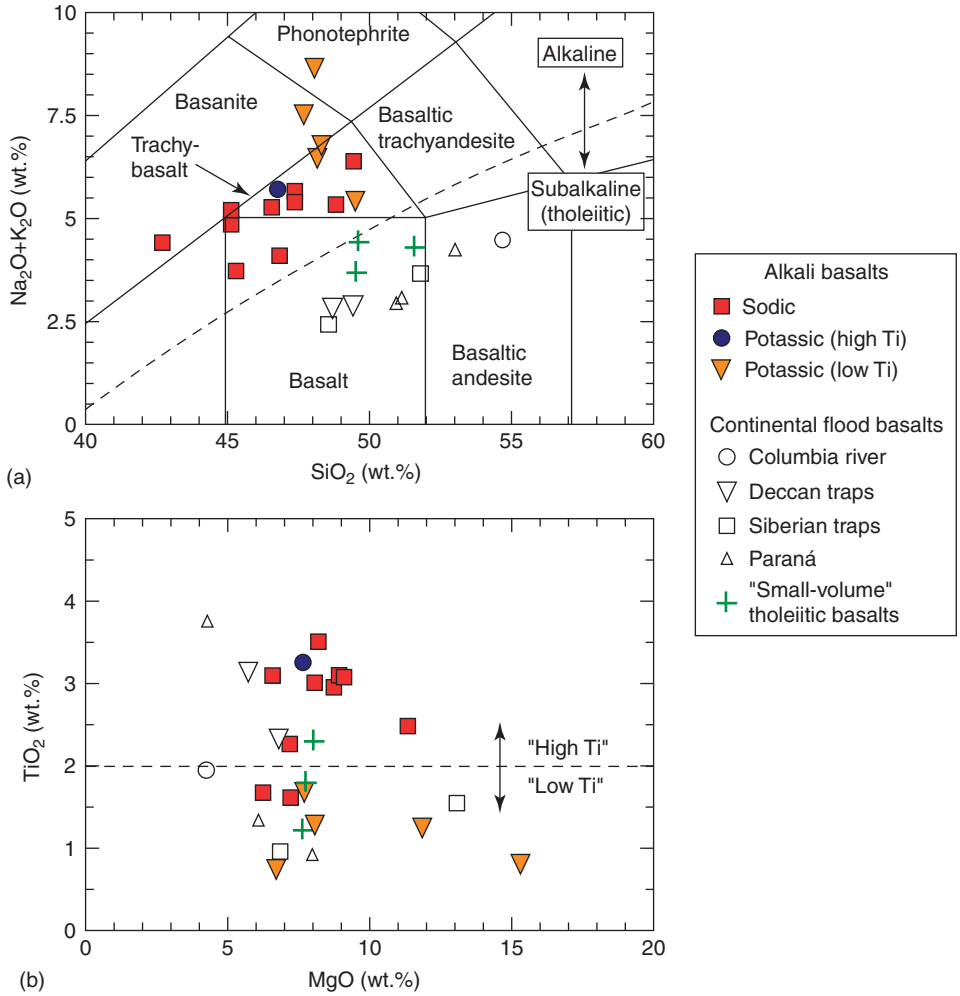

Figure 6 Major element compositions of alkali basalts and CFBs: (a) total alkali elements versus wt.% SiO_2. Dashed line separating alkaline from subalkaline (tholeiitic) basalts from Irvine and Baragar (1971) and (b) wt.% TiO_2 versus wt.% MgO (data from Tables 2 and 3).

3.03.2.5 Factors Influencing Magma Isotopic Compositions

Isotopic data are an essential part of all studies of the source of continental basaltic rocks, and are particularly valuable in attempts to distinguish between sublithospheric and lithosphere sources of basaltic magmas and to assess whether the magmas have interacted with the crust. For example, Cenozoic continental basalts derived solely from sublithospheric sources, are expected to have strontium, neodymium, hafnium, osmium, lead, and/or oxygen-isotopic compositions identical to those of oceanic basalts. For the latter, there is a menu of potential mantle sources, including the high $\varepsilon_{Nd}(=((^{143}Nd/^{144}Nd)_{sample(t)}/(^{143}Nd/^{144}Nd)_{chondrite(t)})-1)\times 10{,}000)$, low $^{87}Sr/^{86}Sr$ upper mantle sources of MORB, and a variety of deeper, isotopically distinct mantle sources that have been defined for OIBs (Figure 7b; Zindler and Hart, 1986; see Chapter 2.03). In terms of their noble gas isotopic compositions, continental basalts derived from the sublithospheric mantle are expected to have $^3He/^4He$ ranging from relatively low and constant values ($R_a = (^3He/^4He)_{sample}/(^3He/^4He)_{atmosphere} \sim 9$) for the upper mantle MORB source to higher and more variable values (R_a from 4 to as high as 43) for the deeper mantle sources of OIBs (Moreira and Kurz, 2001; see Chapter 2.06).

What are the possible isotopic compositions of basaltic magmas derived, at least in part, from the CLM, and can they be distinguished from magmas derived from sublithospheric sources? There are now sufficient isotopic data from continental lithosphere-derived mantle xenoliths to demonstrate that the CLM typically has lower ε_{Nd} (<0), higher $^{87}Sr/^{86}Sr$ ratios (>0.7045), and higher $^{207}Pb/^{204}Pb$ ratios at a

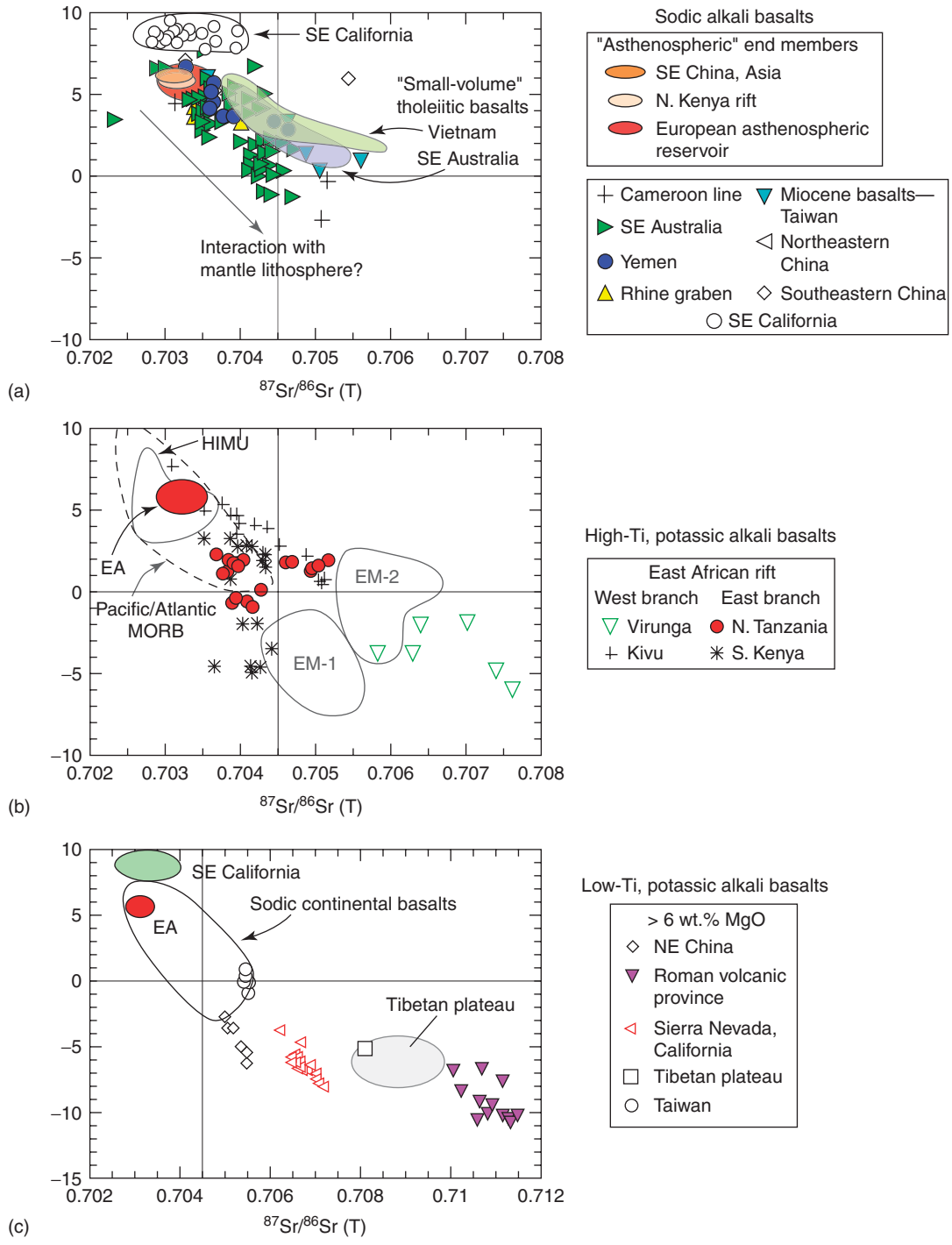

Figure 7 Initial ε_{Nd} versus $^{87}Sr/^{86}Sr$ for continental alkali basalts. (a) Sodic alkali basalts. (b) "High-Ti" potassic alkali basalts. Present-day MORB, EM1, EM2, HIMU mantle sources from Hofmann (1997). (c) "Low-Ti" potassic alkali basalts. EA = European asthenospheric reservoir (data from Table 2).

given $^{206}Pb/^{204}Pb$, compared to sublithospheric mantle (Pearson, 1999; Chapter 2.05) particularly ancient (Precambrian), LREE, and rubidium-enriched lithospheric mantle, or CLM that has been metasomatized by fluids and/or melts derived from subducted oceanic lithosphere and overlying sediments (Nelson, 1992). Basaltic magmas derived from this type of lithosphere inherit these isotopic characteristics and can be distinguished on this basis from many basaltic rocks derived from the sublithospheric mantle.

Osmium-isotopic data also hold promise for distinguishing lithospheric- and sublithospheric-derived basaltic rocks. Archean CLM has been shown to have a nonradiogenic osmium-isotopic composition (present-day $^{187}Os/^{188}Os$ ratio is 0.105–0.129; Shirey and Walker, 1998) relative to sublithospheric mantle (the $^{187}Os/^{188}Os$ is 0.123–0.152), because rhenium is more incompatible than osmium during mantle melting, resulting in a very low Re/Os ratio in Archean mantle, which is probably a product of large degrees of melt extraction (Walker *et al.*, 1989). However, because the Archean mantle is generally refractory, few continental basalts are expected to have exceptionally low $^{187}Os/^{188}Os$. Younger CLM does not necessarily have osmium-isotopic characteristics distinct from the sublithospheric mantle (Lee *et al.*, 2000; Schaefer *et al.*, 2000). Osmium-isotopic data have proved useful, however, in identifying the contribution to continental mafic magmas from olivine-poor, mafic lithologies, because these lithologies have a high Re/Os and, if sufficiently old, can contribute osmium with high $^{187}Os/^{188}Os$ (>0.2) to continental basaltic magmas (Carlson and Nowell, 2001).

Several other isotopic techniques have been brought to bear on the issue of lithospheric versus sublithospheric sources for basaltic rocks, but have not yet been widely applied. Studies of helium isotopes in olivine phenocrysts have demonstrated that CLM-derived magmas characteristically have more radiogenic helium ($R_a \sim 6$) than most sublithosphere-derived basalts (with the exception of HIMU (high μ) basalts), presumably due to a high $(Th + U)/^3He$ ratio in the continental mantle (Reid and Graham, 1996; Dodson *et al.*, 1998). In Quaternary continental basaltic rocks, uranium-series data have also been obtained (Reid and Ramos, 1996). Some workers suggest that large ^{230}Th excesses (10–40%) in some sublithosphere-derived basaltic rocks reflect fractionation of uranium from thorium by garnet and hence a relatively deep derivation for these magmas (Asmerom, 1999).

Light stable-isotope data are relatively rare from intraplate basaltic rocks, in part because the whole-rock stable-isotope compositions of these rocks are susceptible to modification by groundwater during low-temperature, post-emplacement alteration (Taylor, 1968). Laser fluorination oxygen-isotope analyses of unaltered basalt phenocrysts do provide a method for determining magmatic oxygen-isotopic compositions in spite of alteration (Eiler *et al.*, 1997), but the few studies of continental basalts that exist suggest that there is no discernible difference between the oxygen-isotopic composition of lithospheric and sublithosphere mantle (both having $\delta^{18}O \sim 5.3‰$) and magmas derived therefrom (Dobosi *et al.*, 1998).

3.03.2.6 Role of Crustal Contamination

Determining the chemical and isotopic characteristics of primary basaltic magmas is complicated due to the fact that mantle-derived mafic magmas can interact with the continental crust during ascent. Unfortunately, there is no simple recipe for unequivocally recognizing the effects of crustal contamination on the chemical and isotopic compositions of continental basaltic rocks, given the wide range of crustal lithologies that can be assimilated. Interaction between mafic magmas and the upper continental crust, for example, often results in the presence of partially assimilated and disaggregated crustal xenoliths in basaltic rocks. Such rocks are relatively easy to avoid during sampling (Farmer *et al.*, 2002). However, assimilation of lower crust and/or melt derived therefrom can be more difficult to recognize unless sufficient isotopic contrast exists between the primary basaltic magma and the assimilating crust, so that isotopic variations correlate with some index of magma differentiation (e.g., wt.% MgO). To avoid the geochemical effects of such crustal interaction, only the most primitive basaltic rocks in a given location are used to infer the isotopic composition of the original mafic magmas. However, even these magmas may not retain their original isotopic compositions, depending on the chemical and isotopic compositions of the crustal assimilant and the nature of the assimilation process (Reiners *et al.*, 1995; Bohrson and Spera, 2001). In addition, assimilation of pre-existing mafic crust by mafic magmas may produce only minor variations in the chemical and isotopic composition of magma, variations that are only discernible with detailed geochemical studies of multiple rock samples (Glazner and Farmer, 1992).

The problem of crustal contamination is particularly acute for low mg# CFBs and smaller-volume continental tholeiitic basalts, both of which have low trace-element concentrations (see Sections 3.03.3.2.3 and 3.03.3.3). The issue is less critical for many smaller-volume continental rocks, such as kimberlites and alkali basalts, which have much higher abundances of many trace elements. As a result of their high strontium and neodymium content, for example, the isotopic compositions of these elements in kimberlites and alkali basalts are relatively insensitive to modification during crustal contamination. Conversely, the osmium and lead concentration of basaltic magmas

are so low that these isotope systems are particularly vulnerable to modification by interaction with crustal rocks (McBride *et al.*, 2001; Chesley *et al.*, 2002); hence these systems provide relatively sensitive indicators of crustal assimilation.

3.03.3 CONTINENTAL EXTRUSIVE IGNEOUS ROCKS

The above discussion illustrates that the interplay between the thickness and composition of the lithosphere and the composition and potential temperature of the underlying upper mantle control the composition, source, and volumes of Phanerozoic intraplate continental magmatism. Exactly how these factors are related to the production of continental magmas is best illustrated by considering the formation of specific continental igneous rock types.

3.03.3.1 Kimberlites

Kimberlites are small-volume, volatile-rich (CO_2 and/or H_2O), potassic, ultramafic igneous rocks that occur worldwide as dikes, sills, and diatremes within Precambrian cratons. These rocks have been studied extensively, in part because kimberlites represent the primary source of naturally occurring diamonds, but also because they are unusually enriched in LREE, LILE (barium, strontium), and HFSE (niobium, tantalum) and have an ultramafic composition that demands a mantle origin for their parental magmas (Table 1; Mitchell, 1995). Investigations of the origin of their chemical characteristics have been hampered by the fact that kimberlites are clearly hybrid rocks, containing both primary components (i.e., magmatic phenocrysts and groundmass) and xenocrysts (e.g., diamonds) derived from the conduit through which the kimberlitic magma passed during eruption. For example, all kimberlites have unusually high nickel contents (>1,000 ppm; Table 1). These high concentrations do not reflect the values in primary kimberlitic magmas but are due to the incorporation of olivine xenocrysts derived from the disaggregation of peridotite wall rocks (Mitchell, 1995). Another complication arises from the general occurrence of pervasive hydrothermal and/or deuteric alteration in these rocks (Mitchell, 1995).

Despite the difficulty of defining the chemical characteristic of kimberlites, and even in naming the rocks (Woolley *et al.*, 1996), some aspects of the compositions and origins of kimberlites have been broadly accepted. For example, it is now generally accepted that there are two classes of kimberlites, kimberlites (*sensu stricto*) and orangeites (also referred to as "group 1" and "group 2" kimberlites, respectively). The former are CO_2-rich and are characterized by a macrocryst assemblage of olivine, magnesium ilmenite, pyrope, diopside, phlogopite, enstatite, and chromite, set in a fine-grained matrix of olivine and a variety of other minerals, including perovskite and apatite (Mitchell, 1995). Orangeites, in contrast, are H_2O-rich rocks that contain less olivine but significantly more phlogopite than kimberlites, both as macrocrysts and microphenocrysts (hence the original name for these rocks of "micaceous" kimberlites; Dawson, 1967). The distinction between these two kimberlite types was originally recognized amongst the abundant Cretaceous kimberlitic rocks that perforate the Archean Kaapvaal craton in southern Africa, on the basis of the higher initial $^{87}Sr/^{86}Sr$ (0.707–0.711) and low ε_{Nd} values (–6 to –13) of orangeites compared to kimberlites (Figure 8; Smith, 1983). However, while Proterozoic to Tertiary kimberlites worldwide also have relatively high initial ε_{Nd} values (>0), micaceous kimberlites outside South Africa do not always have low initial ε_{Nd} values (cf. the Late Proterozoic Aries kimberlites in western Australia; Edwards *et al.*, 1992). Both kimberlite types have high MgO contents (22–29 wt.% MgO), and low aluminum and silicon (2.3–3.8 wt.% Al_2O_3 and 33–37 wt.% SiO_2), but orangeites have considerably higher K/Na ratios than kimberlites (17–22 versus 3.3–6.2; Table 1). Finally, both kimberlites and orangeites are strongly enriched in LIL, LREE, and HSFE relative to OIB and, unlike typical OIB, have prominent negative potassium anomalies on primitive mantle normalized trace-element plots (Figure 9).

The immediate source of kimberlitic rocks is either CO_2 (for kimberlites) or H_2O (for orangeites) metasomatized peridotite at some depth greater than that of the graphite–diamond transition (~140 km; Figure 1), given the occurrence of xenocrystic diamonds in these rocks (Mitchell, 1995). The high $(La/Yb)_N$ ratios (100–300) of all kimberlitic rocks (Mitchell, 1995), combined with their low aluminum contents, further suggest that kimberlitic rocks represent the products of small degrees of melting (<1%) of an LREE-enriched, garnet-bearing ultramafic rock (Tainton and McKenzie, 1994). A deep source is also consistent with recent experimental data, which suggest that kimberlites equilibrate with carbonated, garnet harzburgite at ~180 km depth (Girnis *et al.*, 1995). Several important questions remain, however, including: Do kimberlites and orangeites

Table 1 Average major element, trace element, and isotopic data for selected orangeites and kimberlites.[a]

	Kimberlite[b] Sierra Leone	*Group 1A kimberlite*[c] global average	*Orangeities*[d] South Africa	*Micaceous kimberlites*[c] global average
Age (Ma)	115		165–110	
n	22	35	114	32
SiO_2	32.5	32.6	32.5	37.0
TiO_2	1.84	1.70	0.88	1.40
Al_2O_3	2.68	2.70	2.27	3.80
MnO	0.17	0.20	0.14	0.20
MgO	27.8	29.1	22.1	26.7
Fe_2O_{3T}	10.9	10.2	7.18	8.9
CaO	7.49	8.30	5.16	6.90
Na_2O	0.26	0.30	0.11	0.20
K_2O	1.63	1.00	2.31	3.30
P_2O_3	0.59	0.70	0.74	1.00
LOI			9.38	
CO_2	4.53	5.30		3.60
H_2O	7.63			
K_2O/Na_2O	6.2	3.3	22	17
Ni	1,177		1,224	
Cr	1,305		1,624	
Zn	66.5		65.3	
Cu			26.8	
Co			80.0	
V	76		104	
Y	10.0			
Sc	14.0		18.8	
Rb	75.0			
Sr	601		1,105	
Cs				
Ba	1,641		3,133	
Zr	179		273	
Hf	5.71		7.00	
Ga	8.40			
Nb	239		115	
Ta	15.72		8.50	
U	3.91		5.00	
Th	26.3		27.5	
Pb	8.29			
La	179		175	
Ce	331		337	
Pr			45.5	
Nd	110		123	
Sm	13.7		14.3	
Eu	3.12		3.44	
Gd			11.4	
Tb	0.71		1.01	
Dy			3.59	
Ho	0.50		0.57	
Er			1.36	
Tm			0.18	
Yb	0.66		1.23	
Lu	0.08		0.14	
$(La/Yb)_N$	175.6		92.2	
$n_i =$ [e]	2			
$^{87}Sr/^{86}Sr$ (T)	0.7040–0.7043		0.7071–0.7109	
ε_{Nd} (T)	−1.4 to +2.7		−6.2 to −13.4	
$^{206}Pb/^{204}Pb$			17.21–18.24	
$^{207}Pb/^{204}Pb$			15.51–15.58	
$^{208}Pb/^{204}Pb$			37.45–38.23	

[a] Major elements reported as weight percent oxides (hydrous), trace elements in ppm. [b] Average of dikes and pipe analyses from Koidu kimberlites, Sierra Leone. Data from Taylor *et al.* (1994, table 1). [c] Global average from Taylor *et al.* (1994, table 4). [d] Data from Swartuggens, Finisch, Bellsbank, and Sover kimberlite localities, as complied in tables 3.1, 3.5, 3.7, and 3.10 in Mitchell (1995). [e] n_i is the number of samples used for radiogenic isotope averages.

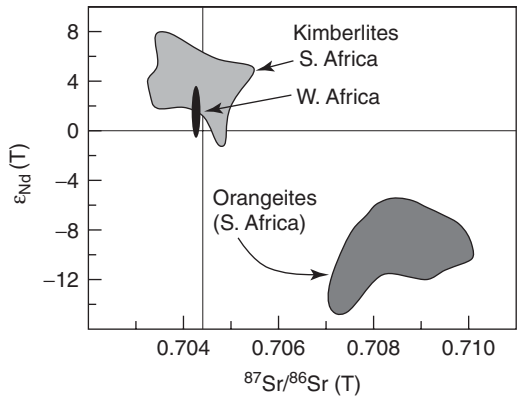

Figure 8 Initial ε_{Nd} versus $^{87}Sr/^{86}Sr$ for African kimberlites and orangeites (group 2 kimberlites). After Mitchell (1995).

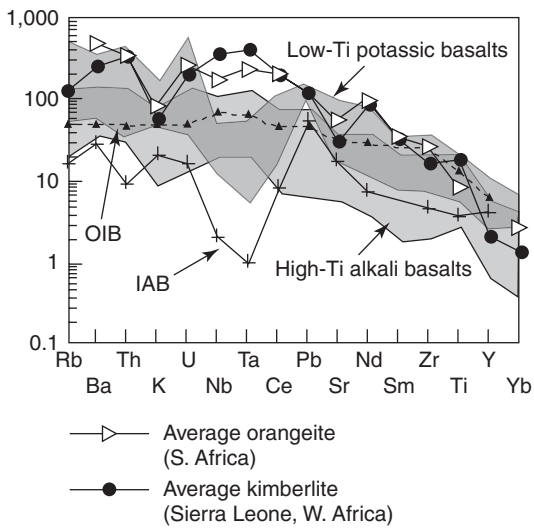

Figure 9 Primitive mantle normalized trace-element abundances for kimberlites and orangeites. Normalization values from Sun and McDonough (1989). Average OIB and IAB data from Sun and McDonough (1989) and McCulloch and Gamble (1991), respectively. High- and low-Ti basalt fields from Figure 11 (data from Table 1).

represent the products of melting in the lithospheric or the sublithospheric mantle? Where did the mantle-metasomatizing fluids originate? What mechanisms are involved in triggering kimberlitic magmatism?

Many authors have suggested that the high ε_{Nd} values of kimberlites (*sensu stricto*) require a source in the convecting, sublithospheric mantle (Smith, 1983; Edwards *et al.*, 1992; Taylor *et al.*, 1994; Mahotkin *et al.*, 2000). The occurrence of majoritic garnet in kimberlites and in entrained diamonds further supports models of an ultra-deep origin of the magmas parental to kimberlites, possibly even in the transition zone (Sautter *et al.*, 1991; Ringwood *et al.*, 1992). In contrast, the low ε_{Nd} of orangeites requires a source in the long-lived (>1 Ga), LREE-enriched mantle, presumably representing the lithospheric mantle. Such a conclusion is consistent with major and trace-element modeling of orangeites by Tainton and McKenzie (1994), who suggested that the aluminum and HREE abundance of these rocks can only be reconciled if they were derived from a mantle that had undergone extensive partial melting, as expected for mantle beneath Archean cratons, that was subsequently metasomatized by fluids enriched in LILE, LREE, and HFSE.

It is important to note, however, that the negative potassium anomalies characteristic of kimberlites and orangeites require that both have equilibrated with the lithospheric mantle containing a residual potassic phase, that is, either phlogopite or potassium-rich amphibole. As a result, the difference in the isotopic composition of kimberlites and orangeites may simply indicate that kimberlites were derived from the lithospheric mantle that was metasomatized at or near the time of kimberlite formation, while a much longer time interval occurred between metasomatism and kimberlitic magmatism in the case of orangeites (Mitchell, 1995).

Exactly what triggers these metasomatic events, or the production of the kimberlite magmatism, remains enigmatic. Several workers have suggested that similarities in the age and spatial patterns of kimberlite magmatism and various hot-spot tracks support the idea that kimberlite magmatism is ultimately related to decompression melting of mantle plumes beneath continents (le Roex, 1986; Heaman and Kjarsgaard, 2000). Others have questioned whether any relationship exists between hot spots and kimberlite magmatism (Mitchell, 1995), particularly because episodes of kimberlite magmatism can occur in the same area, separated in time by hundreds of millions of years (Lester *et al.*, 2001). However, regardless of the trigger mechanism involved in kimberlite magmatism, kimberlites provide evidence that mantle lithosphere, particularly long-lived, deep-rooted, Archean mantle lithosphere, has been periodically metasomatized by $CO_2 \pm H_2O$, LREE, LILE, and HFSE bearing fluids derived from the underlying convecting mantle. The derivation of these fluids from the deep mantle is at least consistent with the similarity in the Nb/U and Ce/Pb ratios of kimberlites and OIB (Figure 5).

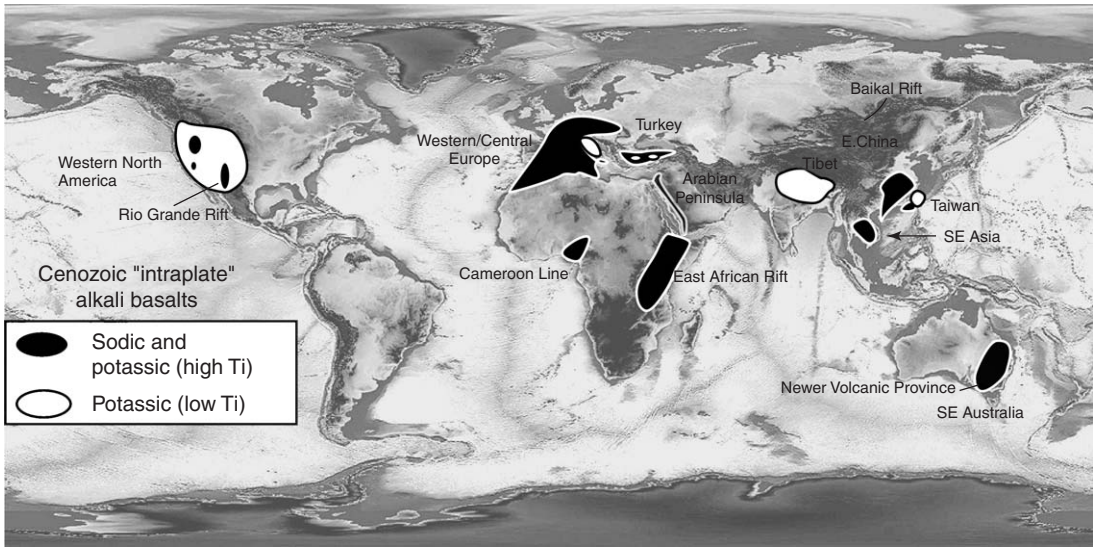

Figure 10 Location of sodic and potassic "intraplate" alkali basalt volcanic fields worldwide. Shown are volcanic fields mentioned in text and for which data are tabulated in Table 2.

3.03.3.2 Alkali Basalts

Cenozoic alkali basalt provinces occur in every continent (Figure 10), often, but not exclusively, associated with active lithospheric extension in localized continental rifts (e.g., Baikal, East African, and Rio Grande rifts) or over broader continental regions (western United States, eastern China, southeast Asia, and southeastern Australia). Continental rifts have long been the focus of studies of continental basaltic rocks, due in part to the large volume of basaltic magmatism that can occur both on and off the rift axis, and because rift magmatism provides a window into the processes involved in rifting and, potentially, in continental breakup (Baldridge *et al.*, 1995). In general, alkaline magmatism occurs early along the axis of rifts, where it can be supplanted later by larger volumes of tholeiitic magmatism (cf. Rio Grande Rift; Baldridge *et al.*, 1995), and along the rift flanks (Thompson and Gibson, 1994). Total magmatic volumes vary substantially from rift to rift. The East African Rift generates the largest volume of magma among present-day rifts ($\sim 2.2 \times 10^5$ km^3 for the Kenya Rift alone; Mohr, 1992).

In broader areas of continental extension, alkali basalts comprise multiple volcanic fields that can collectively cover up to 1,000 km^2 or more, with up to a hundred or more separate volcanoes (Connor and Conway, 2000). The volcanic vents in these regions are often monogenetic (i.e., formed during a single eruptive event), and individual volcanic fields generally produce less than 10 km^3 of volcanic rock during a few thousand years to 5 Myr (Connor and Conway, 2000). Eruptive rates are low, as a result, amounting to <1 km^3 kyr^{-1} (as opposed to the present-day flux of basaltic magma at mid-ocean ridges of ~ 18 km^3 yr^{-1}; Sigurdsson, 2000). Despite their relatively small volume, continental alkali basalt fields have been studied intensively, both because this type of volcanism can be triggered by lithospheric deformation, and hence provides insights into the composition and physical behavior of the deep continental lithosphere, and because they carry mantle xenoliths.

Geochemical studies of alkali basalts have been aided over the past 10–15 years by an explosion in the literature of ICP-MS-based trace-element and radiogenic-isotope data for continental alkali basalts. Representative chemical analyses of the two main alkali basalt groups, sodic and potassic ($K_2O/Na_2O < 1$ and $\geqslant 1$, respectively), are listed in Tables 2a and 2b, respectively, derived from the average composition of lavas at each locality having <51 wt.% SiO_2 and >5 wt.% MgO. No attempt was made to account for crystal accumulation or fractionation, and as a result these averages should not be misconstrued as estimates of "primary" magma compositions. Nevertheless, they do serve to demonstrate the basic chemical distinction between the two alkali basalt varieties.

3.03.3.2.1 Sodic alkali basalts

Cenozoic sodic alkali basalts represent the dominant basalt type in many continental alkali basalt provinces, including northern

Table 2a Average major element, trace element, and isotope data for Cenozoic continental sodic alkali basalts and associated small-volume tholeiitic basalts.[a]

	Sodic alkali basalts										*Tholeiitic basalts*		
	SE Australian[b] Dubbo V.F.	*Arabian Peninsula*[c] Yemen	*Africa-N Tanzania*[d] East African Rift	*West Africa*[e] Cameroon Line		*Turkey*[f] Central Anatolia		*Europe*[g] Rhine garben	*Taiwan*[h]	*NE China*[i]	*Vietnam*[j]	*SE Australia*[k] Newer V.P.	*Taos Plateau*[l] Rio Grande Rift
				Low Sr	*High Sr*	*Early Miocene*	*Late Miocene*						
Age (Ma)	13	<1	<1–8	5–23	5–23	18–20	9.5	18–22	20–23	–15	163–>6.3	<.010–45	3.5–5
n	8	44	23	8	6	3	5	16	3	4	9	7	12
SiO_2	45.3	47.4	46.6	45.1	45.1	48.8	49.4	42.7	47.4	46.8	49.6	51.6	49.5
TiO_2	2.50	2.30	3.02	3.12	3.53	1.64	1.70	3.07	3.12	2.96	2.33	1.81	1.22
Al_2O_3	13.4	16.6	12.4	14.5	14.5	16.6	17.4	13.4	15.6	12.9	14.0	14.3	16.3
MnO	0.19	0.19	0.20	0.17	0.19	0.15	0.16	0.19	0.18	0.96	0.16	0.16	0.18
MgO	11.3	7.2	8.0	8.9	8.2	7.2	6.2	9.1	6.6	8.7	8.1	7.8	7.7
Fe_2O_{3T}	12.9	11.6	13.7	12.4	12.6	9.6	9.0	12.5	2.5	13.2	12.0	11.3	12.1
CaO	9.98	8.74	10.2	10.0	10.1	10.0	9.09	11.6	8.15	9.68	8.88	8.48	9.06
Na_2O	2.79	4.27	3.61	3.62	3.41	3.86	3.94	3.30	3.82	2.78	2.74	3.38	3.15
K_2O	1.00	1.15	1.69	1.49	1.46	1.51	2.50	1.12	1.87	1.35	1.72	0.93	0.56
P_2O_3	0.64	0.62	0.56	0.76	0.97	0.72	0.61	0.76	0.83	0.56	0.57	0.34	0.18
K_2O/Na_2O	0.36	0.27	0.47	0.41	0.43	0.39	0.64	0.34	0.19	0.48	0.63	0.27	0.18
Ni	252	90	195	153	130	153	86	138	99	191	174	153	156
Cr	377	153	334	343	232	193	99	248	108	233	224	266	225
Zn	98.5	81.7	541			74.3	71.0		108		104	112	
Cu	61.4	54.1	109			40.7	40.4			51.4	58.8	61.9	
Co									41.0				51.4
V	211	196	316			133	101	297	205	234		161	157
Y	25.8	34.5	28.3	31.4	35.2	26.7	23.4	29.4	32.3	24.6	24.4	27.1	21.5
Sc	22.0	29.5	19.2			16.0	14.2		17.0	20.6	20.1	19.3	25.3
Rb	23.1	22.1	46.7	38.9	38.0	35.7	42.2	67.7	37.7	24.0	36.3	23.4	54
Sr	765	644	886	959	1470	927	730	926	881	915	740	436	329
Cs												1	
Ba	648	382	670	571	630	805	526	791	730	433	514	278	259

Zr	216	244	283	247	195	183	183	287	295	246	194	147	96
Hf	4.60								6.80	5.48	540	3.37	2.49
Ga	18.3	17.6										20.1	
Nb	62.4	43	90.7	91	74	30	45	82	69.0	69.0	40	24	7
Ta	3.77								4	4.19	2.64		0.45
U		0.75	1.53						1.13	1.41	0.92	1.00	
Th	7.23	3.9	9.91			11.7	9.2		5.20	5.33	4.3	2.9	0.7
Pb		2.45	5.90							5.59		3.4	
La	39.1	33.2	65.6	55.4	48.2	43.1	25.0	62.0	50.3	39.9	32.7	22.1	9.1
Ce	77.9	69.6	143	107	97	85.8	49.1	124	101.5	83	67	40	21
Pr						8.69	5.23			9.58		5.3	
Nd	37.6	34.3	60.0	49.4	50.9	32.3	20.6	56.4	52.3	37.5	31.0	21.5	
Sm	7.56	7.0		9.5	10.7	5.95	4.52	11.7	9.8	7.87	6.8	5.2	3.3
Eu	2.31	2.27		3.01	3.51	1.84	1.54	3.59	3.1	2.49	2.14	1.73	1.16
Gd		6.75		7.75	8.03	5.56	4.69	8.43		6.92		6.08	
Tb	0.957								1.17	0.99	1.03	0.85	0.67
Dy		5.84		5.52	5.65	4.79	4.28	6.01		4.95	4.72	5.26	
Ho	0.986					0.84	0.74			0.85		0.97	
Er		3.25		2.35	2.43	2.28	2.10	2.64		2.08		2.50	
Tm										0.27			
Yb	1.71	2.86		1.85	2.07	2.28	2.06	1.83	2.2	1.46	1.68	1.86	2.07
Lu	0.23	0.43		0.28	0.29	0.39	0.35	0.18	0.32	0.20	0.22	0.27	0.32
$(La/Yb)_N$	14.8	7.5		19.3	15.1	12.2	7.9	21.9	14.8	17.7	12.6	7.7	2.8
n_i = [m]	7	25	19	8	6	3	1	26	3	4	8	7	3
$^{87}Sr/^{86}Sr(T)$	0.7042	0.7035	0.7041	0.7033	0.7035	0.7047	0.7034	0.7036	0.7036	0.7038	0.7046	0.7054	0.7043
$\varepsilon_{Nd}(T)$	0.04	5.14	0.65	4.06	4.17	3.0	6.9	3.67	5.44	4.72	3.35	2.09_n	
$^{206}Pb/^{204}Pb$		18.563	19.255						18.746	18.139	18.533	18.726_n	17.958
$^{207}Pb/^{204}Pb$		15.584	15.587						15.568	15.507	15.594	15.620	15.515
$^{208}Pb/^{204}Pb$		38.624	39.645						38.859	38.233	38.588	38.840	37.482

[a] Major elements reported as weight percent oxides (anhydrous), trace elements in ppm. Average analyses for sodic alkali basalts ($K_2O/Na2O < 1$) constructed from lavas at each locality having < 51 wt.% SiO_2 and > 5 wt.% MgO. [b] Average basanite and alkali olivine basalt, Dubbo volcanic province, eastern Australia. Data from Zhang and O'Reilly (1997). [c] Average Quaternary alkali basalt, western Yemen. Data from Baker *et al.* (1997). [d] Combined average of "older extrusive" and alkali basalts from Loolmalasin, Ketumbeine and Monduli volcanoes in East African Rift, northern Tanzania. Data from Paslick *et al.* (1995). [e] Average, "high" and "low" Sr basanites and alkali basalts from Cameroon Line calculated for rocks with > 6 wt.% MgO. Data from Marzoli *et al.* (2000). [f] Average alkali basalt, Galatia volcanic province, central Anatolia. Data from Wilson *et al.* (1997). [g] Data from Jung and Hoernes (2000). [h] Miocene basalts, northern Taiwan. Data from Chung *et al.* (1995). [i] Data from Chung (1999). [j] Average olivine tholeiite from Buon Ma Thuol and Plieku volcanic areas. Data from Hoang and Flower (1998). [k] Average tholeiitic plains basalt from Newer Volcanic Province, southeastern Australia. Data from Price *et al.* (1997). [l] Average composition of middle member of Servilleta Basalt. Data from Dungan *et al.* (1986). [m] n_i is number of samples used for radiogenic isotope averages. [n] Pb and Nd isotope compositions are average of four olivine tholeiites reported by McBride *et al.* (2001).

Table 2b Average major element, trace element, and isotopic data for Cenozoic continental potassic alkali basalts.[a]

	Africa[b] Virunga V.F. High Ti	*China*[c] Tibetan Plateau Low Ti	*Taiwan*[d] Mt. Tsaoling Low Ti	*Italy*[e] Roman V.F. Low Ti	*Western US*[f] Sierra Nevada Low Ti	*Aegean Sea*[g] Dodecanese V.F. Low Ti
Age (Ma)	<1	<1–13	0–2.8	0.4–0.6	3.5	8.6–12
n	16	6	10	7	27	13
SiO_2	46.8	47.7	48.3	48.1	48.2	49.5
TiO_2	3.26	1.70	0.83	0.78	1.27	1.30
Al_2O_3	13.3	13.2	12.2	15.6	12.6	15.9
MnO	0.18	0.15	0.13	0.14	0.15	0.14
MgO	7.7	7.7	15.3	6.8	11.9	8.1
Fe_2O_3t	12.2	10.7	7.6	8.3	8.9	8.8
CaO	10.3	10.2	7.28	11.1	9.50	10.15
Na_2O	2.37	3.54	1.84	1.16	2.93	2.73
K_2O	3.36	3.97	4.96	7.47	3.52	2.73
P_2O_3	0.56	1.04	1.58	0.55	1.13	0.63
K_2O/Na_2O	1.42	1.12	2.70	6.45	1.20	1.00
Ni	64	102	481	74	271	103
Cr	273	296	1,082	134	665	268
Zn	91.6		49.2	38.1	108	80.4
Cu	35.2		32.9	47.9		
Co	42.2	197	45.2	32.8	40.4	29.9
V	312		154	181		213
Y	27.9	17.0	13.9	35.7	20.6	27.2
Sc	30.4	19.5	27.4	12.5	23.7	27.3
Rb	120	164	1,099	607	69.7	160
Sr	993	3,216	676	1,469	2,223	1,014
Cs	1		116			38
Ba	1,322	2,564	937	1,483	2,927	1,276
Zr	323	585	114	313	341	218
Hf	7.38	10.0	3.20	3.03	7.15	6.66
Ga		17.0	12.5	7.6		
Nb	105		16	14	14	20
Ta	7.36	2.48	0.88	0.30	0.62	1.24
U	3.76		19.1		1.57	6.09
Th	15.3	58.7	20.8	29.6	5.8	19.6
Pb	6.90	30.0	22.9		18.2	
La	93.1	28.2	25.0	95.4	57.0	51.1
Ce	181	465	50	219	122	97
Pr		37	6.03		14.7	
Nd	72.2	273	24.7	95.3	58.9	45.5
Sm	11.9	28.8	4.7	18.7	9.7	9.0
Eu	3.05	7.02	1.14	3.47	2.44	2.39
Gd		12	3.53		6.97	7.09
Tb	1.23	2.2	0.50	1.53	0.82	0.86
Dy		6.30	2.59		3.87	4.57
Ho			0.52		0.68	
Er		2.7	1.47		1.84	2.27
Tm			0.22		0.25	
Yb	2.58	2.20	1.33	2.37	1.44	1.92
Lu	0.38	0.33	0.20	0.40	0.19	0.35
$(La/Yb)_N$	23.4	82.8	12.2	26.1	25.6	17.3
$n_i =$[h]	7	1	10		27	10
$^{87}Sr/^{86}Sr(T)$	0.7069	0.7081	0.7055	0.71007[i]	0.7068	0.7062
$\varepsilon_{Nd}(T)$	–3.93	–5.23	0.25	–8.30	–6.40	–1.62
$^{206}Pb/^{204}Pb$	19.423	18.680		18.76	19.566	
$^{207}Pb/^{204}Pb$	15.758	15.656			15.720	
$^{208}Pb/^{204}Pb$	40.746	39.015			39.197	

[a] Potassic basalts defined herein as having $K_2O/Na_2O > 1$. Average analyses constructed from lavas at each locality having <51 wt.% SiO_2 and >5 wt.% MgO. [b] Average "low silica" basaltic rocks from Muhavura and Gahinga, eastern Virunga Province, Rwanda. Data from Rogers *et al.* (1998). [c] Average calculated for volcanic rocks with >5.5 wt.% MgO. Data from Turner *et al.* (1996a). [d] Average Tsaolingshan rocks. Data from Chung *et al.* (2001). [e] Average calculated for volcanic rocks with >6 wt.% MgO in Sabatini Volcanic District in central Italy. Data from Conticelli *et al.* (1997). [f] Average Pliocene basaltic rock from central Sierra Nevada, California. Data

Europe, eastern Australia, and eastern China (Zhang and O'Reilly, 1997; Zou *et al.*, 2000; Wilson and Patterson, 2001). Sodic alkali basalts are compositionally similar worldwide (Table 2a) and correspond to basalts and trachybasalts with relatively high TiO_2 (~1.5–4 wt.%; Figure 6) and high absolute sodium contents (~2–4 wt.%). The sodic basalts have primitive-mantle normalized trace-element-patterns similar to those of kimberlites and OIBs; they are characterized by relatively high LREE contents, low LILE/HFSE ratios, and, in many cases, a negative potassium anomaly (Figure 11a). Although the sodic basalts show a range of radiogenic isotopic compositions, they typically have high initial ε_{Nd} (>0), low

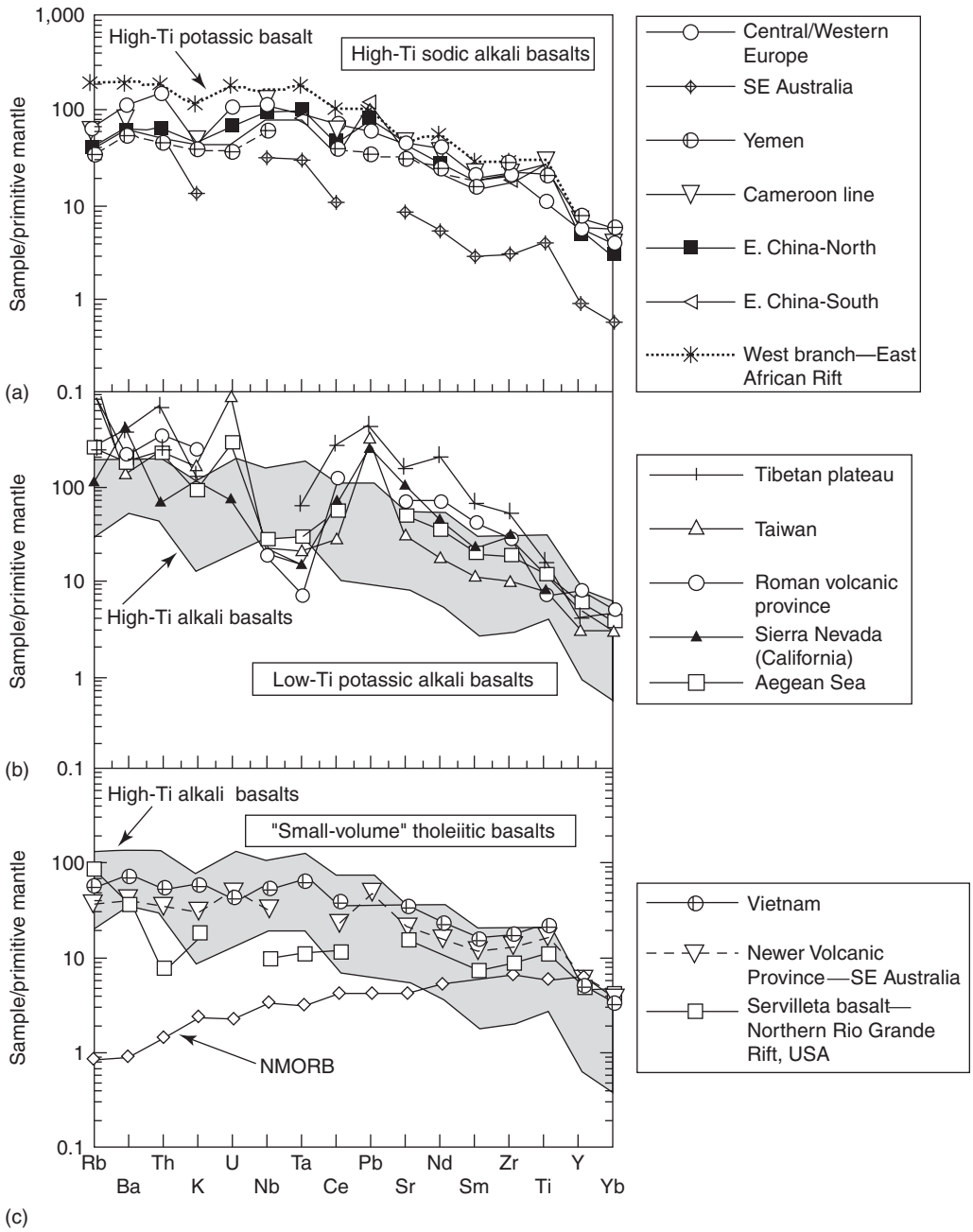

Figure 11 Average primitive mantle normalized trace-element abundances for alkali basalts. Normalization values from Sun and McDonough (1989): (a) high-titanium alkali basalts, including sodic basalts worldwide and potassic basalts from the western branch of the East African Rift; (b) low-titanium potassic alkali basalts; and (c) "small-volume" tholeiitic basalts. N-MORB data from Sun and McDonough (1989) (data from sources given in Table 2).

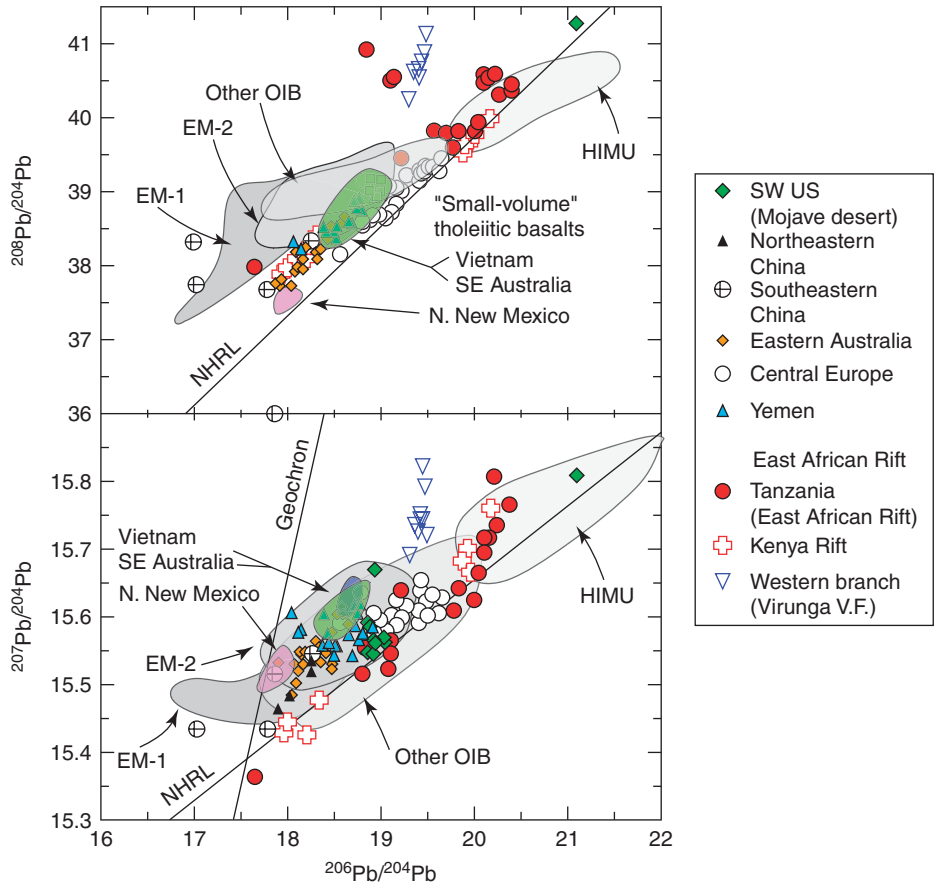

Figure 12 Pb-isotopic compositions for high-Ti sodic alkali basalts worldwide. Data from sources listed in Table 2 and from Zhang *et al.* (2001). NHRL = Northern Hemisphere Reference Line (source: Hart, 1984).

$^{87}Sr/^{86}Sr$ ratios (<0.705), and lead-isotopic compositions that overlap, or parallel (at high $^{207}Pb/^{204}Pb$ for a given $^{206}Pb/^{204}Pb$), the Northern Hemisphere Reference Line (Figure 12).

Both the trace-element and the isotopic composition of sodic basalts are typically cited as evidence that their parental magmas were produced by relatively small degrees of melting (<5 wt.%) of either active (plume) or passively upwelling "asthenospheric" mantle (Fitton and Dunlop, 1985). In western and central Europe, most workers favor models in which Tertiary and Quaternary magmatism is produced by active mantle upwelling (Wedepohl and Baumann, 1999; Wilson and Patterson, 2001). Wilson and Patterson (2001) suggested that domal uplift, lithospheric extension, and Cenozoic volcanism throughout western and central Europe is the result of the impact of five or more relatively narrow mantle diapirs ("hot fingers") derived from a common reservoir at the base of the upper mantle, which is considered by these authors to be akin isotopically and chemically to HIMU OIBs (Figures 7a and 12). Other models have been proposed concerning the role of lithospheric thinning and plume upwelling in producing the temporal and spatial patterns in European alkalic magmatism during the Cenozoic, including channeling of upwelling plume material along thinspots in the European lithosphere (Oyarzun *et al.*, 1997), but most workers agree that mantle lithosphere was not the primary source of the alkalic magmatism. However, interaction between plume-derived melts and low ε_{Nd}, higher $^{87}Sr/^{86}Sr$ mantle lithosphere could have contributed to some of the isotopic heterogeneities observed in the European sodic basalts (Figure 7a; Wilson and Patterson, 2001).

Melting within actively upwelling mantle plumes has been suggested as the ultimate origin of high ε_{Nd} sodic alkali basalts in many other regions around the world, including the northern portions of the East African Rift (Class *et al.*, 1994), western Africa (Cameroon Line; Marzoli *et al.*, 2000), and southeast Australia (McDonough *et al.*, 1985; Zhang and O'Reilly, 1997). In southeast Australia, this conclusion has been

supported by recent osmium-isotopic studies of the Quaternary Newer Volcanic Province, which reveal that sodic alkali basalts there have osmium-isotopic compositions indistinguishable from OIB, again supporting a sublithospheric origin for their parental magmas (McBride *et al.*, 2001). Helium-isotope data are available primarily from sodic basalts in the northern half of Africa (Cameroon Line, Sudan). These basalts have R/R_a values ($\sim$5.1–7.5) consistent with a derivation from an HIMU-type plume source (Barfod *et al.*, 1999; Franz *et al.*, 1999).

While few workers would dispute that the high ε_{Nd} values of sodic alkali basalts require that their parental magmas were dominantly comprised of components recently derived from the sublithospheric mantle, there has been debate whether the sodic basalts represent direct products of sublithospheric mantle melting. An alternative is that these basalts are derived from melting of the lithospheric mantle (particularly "young" high ε_{Nd} mantle lithosphere) that had been metasomatized just prior to basalt formation by incompatible element-enriched fluids/melts derived from small degrees of melting of upwelling asthenosphere. Small melt fractions are likely to freeze within the continental lithosphere (McKenzie, 1989), producing a veined mantle prone to subsequent melting. Such a lithospheric mantle source has been proposed for Quaternary sodic basalts on the Arabian Peninsula (Figure 10), one of the largest alkali basalt fields in the world (Baker *et al.*, 1997). Modeling of very incompatible versus moderately incompatible element ratios (e.g., Ce/Y, Nb/Zr) suggests that the magmas parental to these basalts were derived primarily from $\sim$5% melting of relatively shallow, LREE-enriched, amphibole-bearing, spinel peridotites within the mantle lithosphere (Baker *et al.*, 1997). Given the high ε_{Nd} values for the basalts (average ε_{Nd} $\sim$5:0; Table 2 and Figure 7a), the metasomatism of the lithospheric mantle must have been relatively recent. Baker *et al.* (1997) suggest that the metasomatism occurred during percolation of small melt fractions through the lithosphere. These melts were derived from the high potential temperature and potentially wet Afar plume, which is responsible for the nearby Oligocene flood basalt volcanism. It is interesting to note that the negative potassium anomaly found in the Arabian basalts, which can be taken as evidence of an amphibole-bearing lithospheric mantle source for their primary magmas, is actually common to many continental sodic basalts (Figure 11a), and may indicate that magmatic processes occurring in the mantle lithosphere represent an important step in the generation of all these rocks.

The addition to the lithospheric mantle of small melt fractions derived from the shallow mantle source of MORB (DMM; Zindler and Hart, 1986) is also possible (Ellam and Cox, 1991). A particularly strong case can be made in this regard for sodic basalts in the Cima volcanic field in the southwestern United States. These Late Cenozoic basalts have among the highest ε_{Nd} values of any sodic basalts worldwide (up to 9.5), values that overlap those of Pacific MORBs (Figure 7a; Farmer *et al.*, 1995). Farmer *et al.* (1995) argued that the high ε_{Nd} values of the Cima volcanic field basalts, coupled with their high LREE contents, require that the mantle source of these basalts underwent a recent enrichment in LREE from melts or fluids derived from high ε_{Nd} MORB source mantle. One possibility is that the lithospheric mantle beneath this region was metasomatized by small melt fractions derived from the DMM source. These melts may have been generated during mantle upwelling caused by the Late Cenozoic opening of a slab window through subducting oceanic lithosphere, and do not require the presence of a mantle plume. Such a scenario is not uncommon, and has been suggested for the Antarctic Peninsula and British Columbia (Hole, 1988; Hole *et al.*, 1991). Thus, mantle plumes are not always required for the production of small-volume, sodic alkali basalts.

3.03.3.2.2 Potassic alkali basalts

Cenozoic potassic alkali basalts are less common than their sodic counterparts. They are the dominant basalt type in relatively few regions, such as the Tibetan Plateau (Turner *et al.*, 1996a; Miller *et al.*, 1999), Italy (the famous Roman volcanic province; Conticelli *et al.*, 1997; Peccerillo, 1999), and portions of eastern China (Zhang *et al.*, 1995), Taiwan (Chung *et al.*, 2001), Turkey (Robert *et al.*, 1992), and western North America (Kempton *et al.*, 1991; Figure 10). In each of these areas, the most mafic potassic basalts are characterized by high potassium contents ($\sim$3–7.5 wt.% K_2O) and low titanium contents (0.8–1.7 wt.% TiO_2; Table 2 and Figure 6). The high magnesium contents (>10 wt.% MgO; Table 2b) of many of these basalts clearly require their derivation from an ultramafic mantle source (Turner *et al.*, 1996a). The most distinctive aspect of these rocks, however, is that in addition to their high LILE and LREE abundances, the potassic basalts have pronounced negative niobium and tantalum anomalies, and positive lead anomalies (Figure 11b). In addition, the magmas parental to these rocks were highly oxidizing ($\sim$3–7 log f_{O_2} greater than typical "asthenospheric"

mantle) and contained high volatile contents (H_2O and F > 2 wt.%; Feldstein and Lange, 1999). All these chemical characteristics are similar to those of modern IABs (McCulloch and Gamble, 1991). As a result, while none of the low-titanium potassic basalts listed in Table 2b formed during active subduction, the mantle sources of these rocks appear to have been metasomatized by hydrous, high-potassium, low-HFSE fluids derived from the dehydration of subducted oceanic lithosphere. Such an origin is consistent with the fact that many potassic basalts, including the basalts in the Tibetan Plateau, Taiwan, Italy, and the western United States, erupted soon after the cessation of subduction beneath the underlying continental lithosphere.

The primary exception to a "post-subduction" origin for mantle sources of potassic basalts are those occurring in the southern portions of both the eastern and western branches of the East African Rift (Furman, 1995; Paslick *et al.*, 1995; Rogers *et al.*, 1998; Furman and Graham, 1999), an area that has not witnessed subduction for at least 500 Myr (Petter, 1991). However, unlike potassic basalts elsewhere, these basalts have high titanium contents (> 2 wt.% TiO_2; Table 2) and lack negative HFSE anomalies (Figure 11a). Instead, they have trace-element patterns similar to those of kimberlites, OIBs, and sodic continental alkali basalts (Paslick *et al.*, 1995).

From an isotopic perspective, both low- and high-titanium potassic basalts are distinct from sodic basalts in having generally lower ε_{Nd} values (~0 to –8), higher $^{87}Sr/^{86}Sr$ ratios (~0.704–0.708; Figures 7b and 13) and more variable lead-isotopic compositions (Figure 13). The low ε_{Nd} values of the potassic basalts are generally taken as evidence that the basalts were derived from ancient (i.e., Precambrian age), LREE-enriched, lithospheric mantle sources (Rogers *et al.*, 1998; Miller *et al.*, 1999). It is important to note, however, that because of the mobility of lead and strontium in slab fluids, and lead, strontium, and neodymium in melts produced from subducted oceanic lithosphere and overlying sediments (Pearce and Peate, 1995), mantle metasomatized above subducted lithosphere could have low ε_{Nd}, high $^{87}Sr/^{86}Sr$, and variable lead-isotopic composition as the result of addition of such components from the subducted lithosphere itself (Nelson, 1992). As a result, the isotopic composition of the low-titanium potassic basalts do not necessarily require melting in the ancient lithospheric mantle but could represent melting of the young lithospheric mantle (Farmer *et al.*, 2002). The African high-titanium potassic basalts, in contrast, represent melting of the ancient

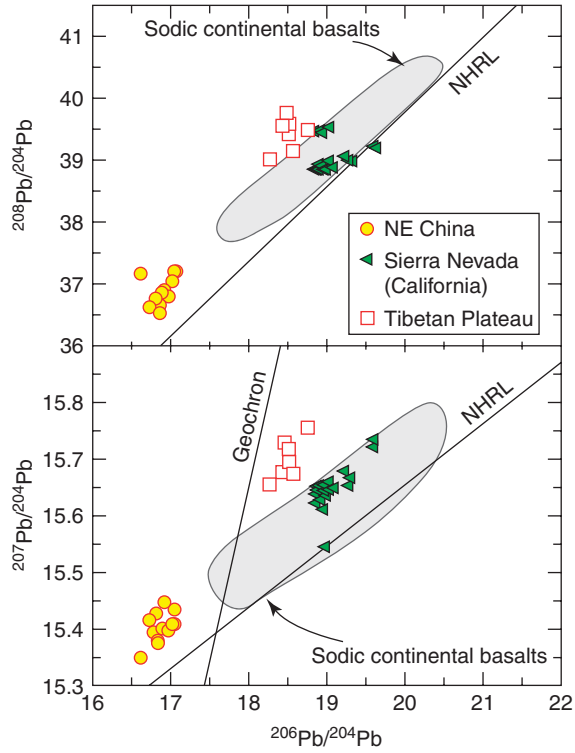

Figure 13 Pb-isotopic compositions for low-Ti potassic alkali basalts worldwide. Data from sources listed in Table 2.

lithospheric mantle originally metasomatized by HFSE-rich fluids that were ultimately derived from a deeper portion of the sublithospheric mantle. This scenario is similar to that suggested for the metasomatized sources of orangeites.

Given the relatively low melting temperature of hydrated mantle of any age (Figure 3) (Harry and Leeman, 1995), it is not surprising that potassic continental basaltic magmatism derived from such mantle can follow closely the cessation of subduction. But what triggers the magmatism? In the Tibetan Plateau, several authors have suggested that Cenozoic potassic magmatism is derived from relatively shallow lithospheric mantle (Turner *et al.*, 1996a; Chung *et al.*, 1998). This mantle was apparently heated and melted as a result of the removal of the originally underlying lithospheric mantle via convective erosion by the asthenosphere, or "delamination," shortly after collision of India and Asia. Similarly, in the Sierra Nevada of the western United States, the abrupt onset and short duration of Cenozoic potassic magmatism has been taken as evidence that shallow ($\sim$40 km deep), hydrous lithospheric mantle melted in response to abrupt delamination of the underlying lithosphere (Farmer *et al.*, 2002). Therefore, potassic magmatism may provide information regarding the timing and extent of major deformational events in the deep-continental lithosphere, events that led not only to the potassic magmatism but also to major episodes of continental mountain building (i.e., the Tibetan Plateau and the Sierra Nevada).

3.03.3.2.3 Small-volume tholeiitic basalts

Cenozoic alkalic basalt volcanism worldwide is often accompanied by the eruption of tholeiitic (subalkaline) basalts. In some continental regions, such as eastern Australia, tholeiitic basalts can comprise up to 50% or more of the total erupted material (Johnson *et al.*, 1989). In southeast Asia, where plateaus dominantly comprise tholeiitic basalts covering an area of $\sim 2.3 \times 10^4\,km^2$ (Figure 10), a total of $\sim$8,000 km^3 of basalt erupted during the Late Cenozoic, at rates estimated at $\sim 3\,km^3\,kyr^{-1}$ (Hoang and Flower, 1998). Although significant, even these magmatic volumes and eruptive rates are several orders of magnitude smaller than those of the typical CFBs (see following section).

These "small-volume" tholeiitic basalts are compositionally heterogeneous in any given volcanic area. They range in composition from olivine to quartz tholeiites, with phenocrysts assemblages of olivine $\pm$ clinopyroxene $\pm$ plagioclase $\pm$ Fe–Ti oxides (Dungan *et al.*, 1986; Price *et al.*, 1997; Wedepohl, 2000). Olivine tholeiites are generally considered the most primitive of the tholeiitic basalts, but their relatively high SiO_2 contents ($\sim$50 wt.%; Table 2a and Figure 6) and low Mg numbers ($< \sim 0.66$) indicate that even these rocks crystallized from magmas that had undergone significant differentiation prior to eruption, most likely through the removal of early formed olivine crystals (Dungan *et al.*, 1986). Such protracted magmatic differentiation not only obscures the original chemical composition of the parent magmas, but also suggests that these magmas may have resided sufficiently long in the continental crust to experience substantial crustal contamination. A slow ascent through the crust is consistent with the general lack of entrained mantle-derived xenoliths in the tholeiitic rocks. The high rubidium, barium, and potassium contents, relative to thorium (Figure 11c), of the Servillleta basalts at the northern end of the Rio Grande Rift in the southern United States (Figure 10), along with their low $^{206}Pb/^{204}Pb$ ($\sim$18) and $^{208}Pb/^{204}Pb$ ($\sim$37.5) ratios (Figure 12), have all been taken as evidence that these rocks interacted significantly with the lower continental crust in this region (Dungan *et al.*, 1986). The trend toward higher $^{87}Sr/^{86}Sr$, at a given ε_{Nd} value, for "small volume" Cenozoic tholeiitic rocks in both the Newer Volcanic Province in SE Australia and in Vietnam (Figure 7a) can also be interpreted as evidence of interaction with low ε_{Nd}, high $^{87}Sr/^{86}Sr$, continental crust. In addition, the osmium-isotopic compositions of tholeiitic basalts in the Newer Volcanic Province are considerably more radiogenic and variable than the compositions of contemporaneously erupted alkali basalts (γ_{Os} $((^{187}Os/^{188}Os)_{sample(t)}/(^{187}Os/^{188}Os)_{chondrite(t)}) - 1) \times 100 = 42$–$251$ versus 5.6–7.6), and so provide evidence that the olivine tholeiites assimilated continental crust in amounts up to 2.5% of original magma mass (McBride *et al.*, 2001).

The fact that "small-volume" tholeiites may have generally interacted with continental crust considerably complicates the issue of determining the sources of their parental magmas on the basis of chemical and isotopic data. As a result, while many workers accept the conclusion that "small volume" tholeiitic basalts represent larger degrees ($\sim$10%) of partial melting of peridotite than alkali basalts and last equilibrated at shallow levels ($< \sim$45 km) in the mantle (Hoang and Flower, 1998; DePaolo and Daley, 2000; Wedepohl, 2000), there is no consensus regarding the relative roles of CLM and sublithospheric mantle in their generation. In the northern half of the Rio Grande

Rift, for example, some authors have suggested that the relatively high $^{87}Sr/^{86}Sr$ ($\sim$0.705) and low ε_{Nd} ($\sim$0 to +5; Baldridge *et al.*, 1991) of tholeiitic basalts require a source in the lithospheric mantle (Perry *et al.*, 1987). Others have argued for melting in upwelling asthenosphere, potentially initiated in the garnet stability field (Beard and Johnson, 1993), and subsequent interaction with either continental crust, or lithospheric mantle (Thompson and Gibson, 1994). Interaction between tholeiitic magmas and mafic veins within the lithospheric mantle has also been proposed to account for the radiogenic osmium-isotopic compositions of Late Cenozoic high-alumina tholeiites in the northwest United States (Hart *et al.*, 1997). There is a similar diversity of opinion regarding the sources of tholeiitic basalts in the Newer Volcanic Province, both lithospheric (Price *et al.*, 1997) and sublithospheric (McDonough *et al.*, 1985) sources having been proposed.

Distinguishing between the lithospheric and sublithospheric mantle as a source for the "small-volume" tholeiites ultimately involves assessing whether lithospheric mantle beneath a given area is sufficiently fertile to spawn basaltic magmas at all, let alone basalts of the appropriate chemical and isotopic compositions and, if not, whether the CLM has been eroded and/or thinned to allow asthenospheric mantle of a given potential temperature to rise to the shallow depths required to produce the observed compositions and volumes of tholeiitic magmatism. The conflicting interpretations of the origin of "small-volume" tholeiitic basalts worldwide make addressing these issues a difficult task. A similar difficulty exists in determining the sources of large-volume tholeiitic basalts found on continents, as described in the following section.

3.03.3.3 Continental Flood Basalts

LIPs are the most massive short-lived igneous events on Earth (Coffin and Eldholm, 1994). These events produce large volumes of mafic lavas and intrusive rocks, and are responsible for the formation of many oceanic plateaus (see Chapter 3.16), volcanic passive continental margins, and CFBs. Post-250 Ma CFBs, because of their better preservation and potential link to Phanerozoic mass extinctions (Renne *et al.*, 1995), are the most thoroughly studied of continental LIPs (Hooper, 2000). The archetypal Mesozoic and younger CFBs include those of the Paraná (Brazil)–Etendeka (NW Namibia) Province, the Deccan Traps, the Siberian Traps, the Karoo (Lesotho, S. Africa)–Ferrar (Antarctica)–Tasmanian Province, and the Columbia River basalts (NW USA; Figure 14). Estimates of eruptive volume of flood basalt provinces are huge. They range from a low of $\sim 2 \times 10^5\,km^3$ for the Columbia River basalts to more than $2 \times 10^6\,km^3$ for the Siberian Traps (Hooper, 2000; Reichow *et al.*,

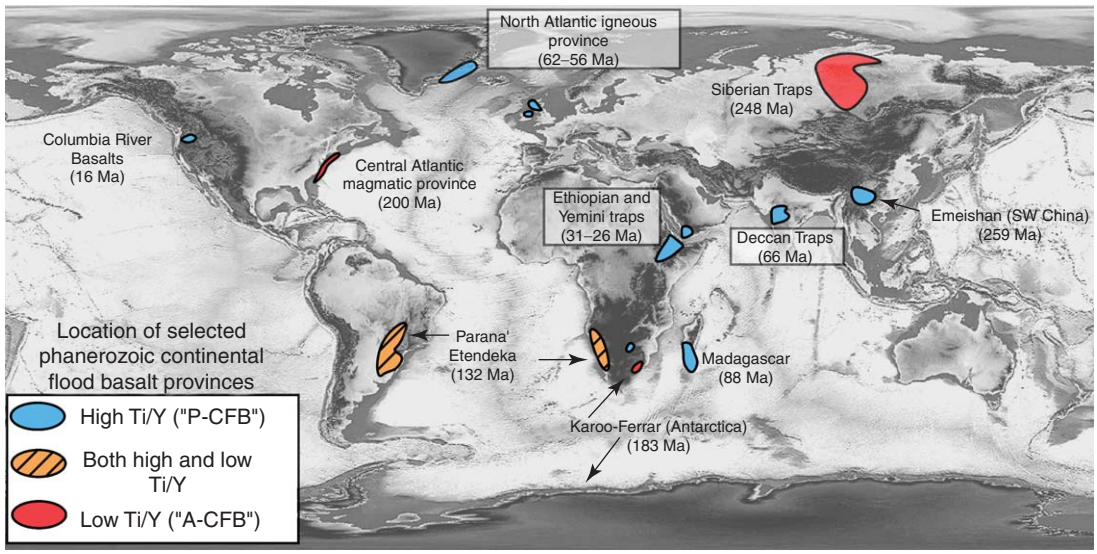

Figure 14 Locations of selected major Phanerozoic CFBs worldwide. References as in Table 3, with exception of Madagascar (Storey *et al.*, 1997), Emeishan (Chung and Jahn, 1995; Zhou *et al.*, 2002), North Atlantic Igneous Province (Saunders *et al.*, 1997), Ethiopian and Yemeni traps (Menzies *et al.*, 1997; Pik *et al.*, 1999), and Central Atlantic magmatic province (CAMP) (Hames *et al.*, 2000). The separation of CFB provinces into high Ti/Y ("P" or "plume" type) and low Ti/Y ("A" or "arc" type) from Puffer (2001). However, most provinces include examples of both "types" of basaltic rocks (cf. the Paraná-Etendeka provinces). A more complete compilation of terrestrial LIPs can be found in Ernst and Buchan (2001).

2002). Even more remarkable is the relatively short time span apparently involved in the eruption of the bulk of the CFB in a given province, which, according to some estimates, could be as short as ~1–3 Ma (Renne and Basu, 1991; Renne *et al.*, 1992; Courtillot *et al.*, 1999). This implies eruption rates as high as $10^3\,km^3\,kyr^{-1}$.

Compositionally, CFBs are all tholeiitic basalts with a simple phenocryst assemblage consisting of plagioclase, clinopyroxene, and Fe–Ti oxides (Hooper, 2000). The high Fe/Mg ratios for these rocks (wt.% Fe_2O_{3T}/MgO ~1–3) and their relatively high silicon contents (wt.% $SiO_2 = 49–57$; Table 3 and Figure 6) are generally interpreted as evidence that CFBs are not primary mantle melts but represent magmas that have undergone significant magmatic differentiation, presumably through crystal–liquid separation, prior to eruption. However, Lange (2002) has demonstrated, at least in the case of the Columbia River basalts, that iron-rich CFB magmas are too dense to ascend through the continental crust unless the pre-eruptive volatile contents of these magmas are much higher than generally assumed ($CO_2 + H_2O$ of at least 4 wt.%). If so, CFB must be an even more significant source of atmospheric volatiles, including greenhouse gases, than previously recognized, and phenocrysts present in CFB may have been produced during eruption and degassing of their parental magmas, in which case the role of crystal fractionation in producing the apparently evolved compositions of CFB is called into question (Lange, 2002).

Despite their similar major-element compositions, CFBs show a wide range of trace-element and isotopic compositions. They can be divided into two groups based on their trace- and minor-element abundances: the "high-titanium" (>2 wt.% TiO_2) and "low-titanuium," or, alternatively, high-Ti/Y (>310) and the low-Ti/Y groups (see Peate, 1997 and references therein, and Hornig, 1993). The "high-titanium" CFBs, such as the Deccan Traps, have low LIL/HFSE ratios similar to, albeit with lower overall LIL and LREE abundances, those of ocean island basalts, kimberlitic rocks, and sodic alkali basalts. "Low-titanium" (or low-Ti/Y) CFBs, such as some CFB flows within the Siberian Traps and the Paraná provinces, have prominent depletions in HSFE relative to LIL, and high lead contents similar to the relative trace-element abundances of IABs and potassic alkali basalts (Figure 15). In general, the "high-titanium" CFBs also tend to have higher initial ε_{Nd} and lower $^{87}Sr/^{86}Sr$ than their "low-titanium" counterparts (0 to +4.5 versus –3 to –8, and 0.7045–0.7066 versus 0.706–0.708, respectively; Table 3; Figure 16).

The previous discussion of kimberlites and alkali basalts indicates that it would be reasonable to suggest that "high-titanium" CFBs represent melts of upwelling asthenosphere (or young lithospheric mantle recently metasomatized by fluids/melts derived thereof), while "low-titanium" CFBs are the products of melting of Precambrian or younger lithospheric mantle that had been metasomatized by fluids/melts derived from subducted oceanic lithosphere and/or sediments (Puffer, 2001). However, it is important to note that any model for the formation of CFB must also take into account the large volume of magma generated during the formation of CFBs and the fact that CFBs are not primary magmas and may have differentiated within, and interacted extensively with, the continental crust. As a result, suggesting that high- and low-titanium CFBs are derived sublithospheric and lithospheric sources, respectively, is not as reasonable an assertion as it was for the much smaller-volume kimberlites and alkali basalts.

The large volume of magma represented by CFBs, and LIPs, in general, favor models of CFB generation within mantle plumes with potential temperatures up to 300 °C higher than typical upper mantle (Morgan, 1971). Upwelling of such mantle plumes, particularly when accompanied by lithospheric thinning, leads to thick mantle melting columns that extend to shallow mantle depths (Figure 1). This provides the conditions required to produce the large volumes of tholeiitic magmas represented by CFBs (McKenzie and Bickle, 1988). From a geochemical standpoint, melting of an upwelling mantle plume can account for the chemical and isotopic composition of "high- titanium" CFBs, most notably the ~64 Myr Deccan Traps (Figures 15 and 17; Puffer, 2001). Many "high-titanium" Deccan Trap flows have trace-element and isotopic compositions consistent with derivation by decompression melting of the Reunion plume (cf. Mahoney, 1988). The high $^3He/^4He$ ratios of mafic alkaline rocks associated with the Deccan flood basalts (R_a ~13:9) are similar to those of oceanic volcanic rocks derived from the Reunion plume. This observation also supports the hypothesis that the impingement of this plume on the base of the Indian lithosphere was responsible for the CFB magmatism (Basu *et al.*, 1993).

A plume source, with or without an upper mantle (MORB source) contribution, is also likely for some of the Siberian CFBs (Sharma, 1997), particularly the "high-titanium," older Gudchiniksy basalts (Table 3) and associated highly magnesian (up to 22 wt.% MgO) picrites, which have high ε_{Nd} values (~+4)

Table 3 Major element, trace element, and isotopic compositions of continental flood basalts.[a]

	Columbia River Basalts[b] NW US High Ti[f]	*Deccan Traps*[c]						
	Mahabaleshwar High Ti	*Deccan Traps*[c] Kolhapur Low Ti	*Siberian Traps*[d]	Nadezhdinsky High Ti	*Siberian Traps*[d] Gudchikhinsky Low Ti	*Paraná*[e] *Esmeralda High Ti*	*Paraná*[e] Gramado Low Ti	*Paraná*[e] Urubici High Ti
Age (Ma)	16	60	60	250	250	127–137	127–137	127–137
n	36	6	18	9	7	1	1	1
SiO_2	54.7	49.5	48.7	51.8	48.5	51.1	50.9	53.0
TiO_2	1.97	2.34	3.16	0.97	1.58	1.37	0.95	3.76
Al_2O_3	14.0	14.1	13.4	15.1	11.6	13.8	14.9	12.9
MnO	0.25	0.18	0.23	0.17	0.17	0.21	0.17	0.19
MgO	4.20	6.9	5.7	6.8	13.0	6.1	8.0	4.3
Fe_2O_{3T}	12.1	13.4	15.1	10.8	13.8	13.4	10.3	12.7
CaO	7.99	10.45	10.28	10.45	8.69	10.73	11.61	8.30
Na_2O	3.06	2.51	2.51	2.37	2.12	2.55	2.44	2.57
K_2O	1.44	0.40	0.34	1.35	0.38	0.54	0.51	1.70
P_2O_3	0.35	0.23	0.39	0.14	0.15	0.16	0.16	0.58
K_2O/Na_2O	0.47	0.16	0.14	0.57	0.18	0.21	0.21	0.66
Ni	28	134	69	59	589	58	99	58
Cr	39		151	137	595	94	307	75
Zn	11.3	109	124	84.3	112	89.0	72.0	107
Cu	39.6	142	266	60.8	105	169	99.0	267
Co				41.3	64.7	50.0	44.0	36.0
V	332		405			323	221	343
Y	35.6	30.0	42.0	27.0	24.0	29.0	23.0	39.0
Sc	34.4			32.2	24.1	42.0	40.0	29.0
Rb	35.6	7.0	13.0	40.2	14.7	19.0	10.0	30.0
Sr	323	283	234	259	307	163	216	764
Cs	0.93			0.77	1.40			

Ba	546	175	123	412	110	163	243	600
Zr	165	138	198	129	102	100	92	307
Hf	4.24	3.70	5.40	2.94	2.46	2.71	2.15	7.97
Ga	20.9					21.0	17.0	26.0
Nb	13.7	15	17	11	14	6	9	27
Ta	0.92	0.80	1.30	0.48	0.47	0.37	0.50	1.92
U	1.08			0.99	0.36	0.71		1.34
Th	3.71	2.1	2.3	2.92	1.07	1.75	2.04	4.25
Pb	6.94			4.72	1.26		3.39	
La	22.1	16.5	17.5	16.7	7.94	8.35	10.6	42.5
Ce	44.6	37.6	43.8	36.0	20.4	20.8	22.9	90.4
Pr	5.79							
Nd	25.2	23.2	29.2	17.5	13.5	14.5	12.8	54.3
Sm	6.45	5.7	7.7	4.01	3.63	3.97	3.18	11.6
Eu	2.01	1.74	2.47	1.10	1.24	1.41	1.11	3.53
Gd	6.56			4.09	3.91			
Tb	1.12			0.65	0.62	0.90	0.63	1.54
Dy	6.90							
Ho	1.40			0.93	0.74			
Er	3.99							
Tm	0.55			0.39	0.27			
Yb	14.43	2.47	3.68	2.39	1.55	2.92	2.09	2.99
Lu	0.54	0.39	0.58	0.35	0.21	0.47	0.35	0.44
$(La/Yb)_N$	0.99	4.32	3.08	4.51	3.31	1.85	3.28	9.20
Ti/Y	332	468	451	216	395	283	248	578
n_i = [g]	31	6	18	5	3	1	1	1
$^{87}Sr/^{86}Sr$ (T)	0.7063	0.7066	0.7045	0.7078	0.7063	0.7058	0.7073	0.7060
ε_{Nd}(T)	1.64	–0.18	4.54	–8.10	3.20	0.70	–3.80	–3.40
$^{206}Pb/^{204}Pb$[h]	18.911	18.370	17.820	18.296	18.726	18.661 ($n=13$)	18.696 ($n=11$)	
$^{207}Pb/^{204}Pb$	15.614	15.520	15.421	15.570	15.570	15.639	15.649	
$^{208}Pb/^{204}Pb$	38.788	38.880	28.244	38.341	38.341	38.706	38.824	

[a] Major-element compositions reported as weight percent oxides (anhydrous), trace-element abundances in ppm. [b] Grande Ronde basalt average. Data from Hooper and Hawkesworth (1993). [c] Average compositions of Mahabaleshwar and Kolhapur basalts from Lightfoot *et al.* (1990). [d] Average compositions of Nadezhdinsky and Gudehikhinsky basalts from Wooden *et al.* (1993). [e] Representative analyses from Esmeralda (sample # DSMO6), Gramado (#DUP30), and Urbici (#DUP35) from Peate (1997). [f] High- and low-Ti basalts defined following Peate (1997), the former having wt.% $TiO_2 > \sim 2$ and $Ti/Y > 310$. [g] n_i number of samples used for radiogenic isotope averages. [h] Pb isotopic compositions are measured values.

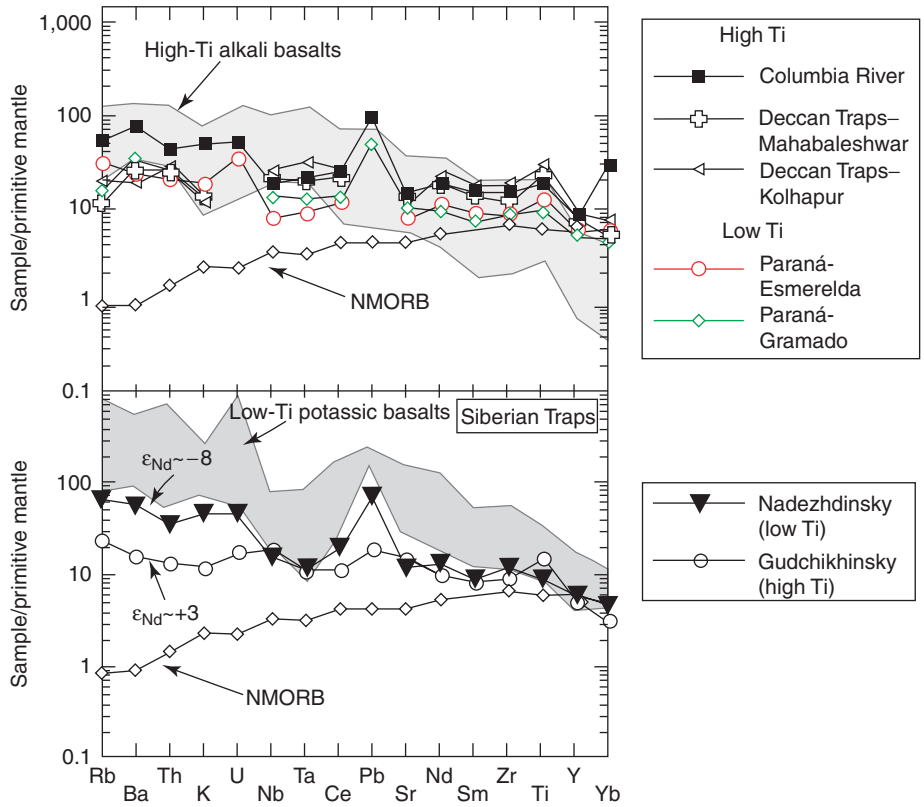

Figure 15 Primitive mantle normalized trace-element abundance for CFBs (data from Table 3). NMORB data from Sun and McDonough (1989).

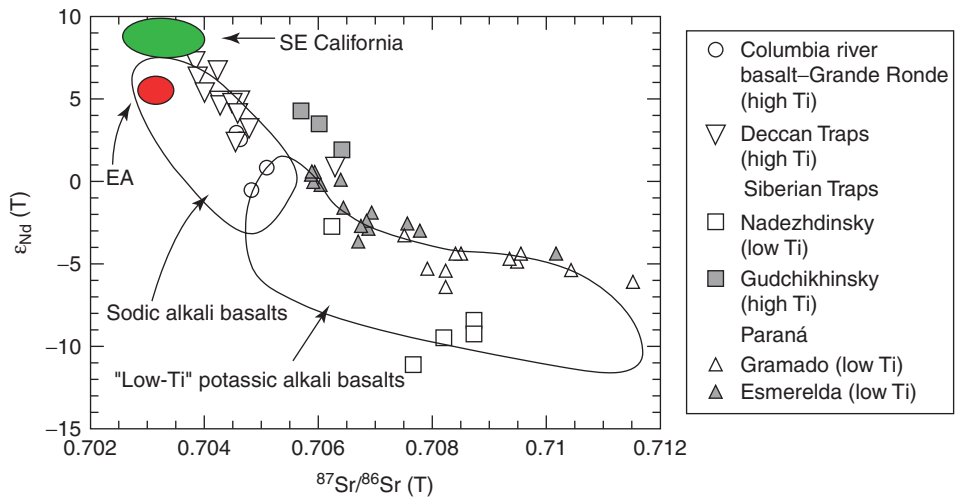

Figure 16 Initial ε_{Nd} versus $^{87}Sr/^{86}Sr$ for CFBs. EA = European Asthenospheric Reservoir (Wilson and Patterson, 2001) (data from Table 3).

and low LIL/HFSE ratios (Figures 15 and 17; Wooden *et al.*, 1993). Picrites are rare, highly magnesian lavas (>12 wt.% MgO) that occur early in the eruptive sequence of several CFBs (Gibson, 2002) and are interpreted as the products of mantle melting at pressures above ~3 GPa (Herzberg and O'Hara, 1998). In the Siberian Traps, picrites also have high initial γ_{Os} (3.4–6.5; Horan *et al.*, 1995), and olivine phenocrysts within early alkaline mafic and ultramafic volcanic rocks elsewhere in the Siberian Traps have high $^{3}He/^{4}He$ (up to ~13 times the atmospheric values; Basu *et al.*, 1995). Both observations are consistent with the derivation of these rocks from melting in a mantle plume that is compositionally similar to those

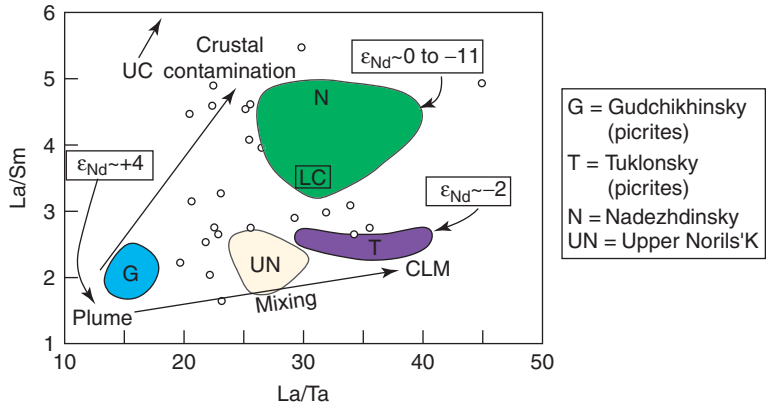

Figure 17 La/Sm versus La/Ta for the Siberian Traps. UC = upper crust, LC = lower crust. Reproduced by permission of American Geophysical Union from Lassiter and De Paolo (1997).

spawning some OIBs. Even the major- and trace-element compositions of the low-titanium Putorana basalts, which represent 90% of the Siberian Trap volcanism, can be modeled as requiring the derivation of these rocks from primary picritic magmas generated by 12–18% melting of an upwelling mantle plume at shallow (spinel stability field) depths in the sublithospheric mantle beneath a thinned lithosphere (Basu *et al.*, 1998).

Picritic rocks are also of interest in CFB provinces because of their compositional heterogeneities. Some of the early picrites have very high iron contents, inconsistent with their derivation by melting of peridotite, even at great depth (Gibson *et al.*, 2000). The high iron contents are instead interpreted as evidence of compositional heterogeneities in the plume head rising beneath continents. The high iron content is taken as evidence of melting of mafic lithologies, or of peridotite metasomatized by melts derived therefrom (Cordery *et al.*, 1997; Korenaga and Kelemen, 2000; Gibson, 2002).

Regardless of the degree of chemical heterogeneity, derivation of low-titanium CFBs by direct melting of an upwelling plume is difficult to reconcile with their high-LIL/HFSE ratios, particularly those CFBs with ε_{Nd} values <0 (Figure 16), because these chemical and isotopic characteristics are so distinct from those of plume-derived OIBs. A lively debate has developed in the literature about whether the isotopic and trace-element compositions of these CFBs reflect derivation, at least in part, from the lithospheric mantle, metasomatized by subduction-related fluids/melts, or whether it reflects extensive crustal contamination of plume-derived magmas (Ellam and Cox, 1991; Hergt *et al.*, 1991; Arndt and Christensen, 1992; Lassiter and DePaolo, 1997). Low-titanium, low-ε_{Nd} CFBs from the Norils'k area of the Siberian Traps, for example, have been interpreted as the products of extensive interaction between plume-derived magmas and continental crust during magmatic differentiation (Wooden *et al.*, 1993). Others, however, have noted that the Norils'k area "low-titanium" (and high-La/Ta) CFBs and picrites do not have high La/Sm ratios, as would be expected from interaction with high La/Sm upper crust (Figure 17; Lassiter and DePaolo, 1997). The low-titanium basalts are instead attributed to mixing between high-titanium, high-ε_{Nd} plume-derived magmas, and a low-ε_{Nd}, high-La/Ta component derived presumably from metasomatized portions of the lithospheric mantle. A similar model was proposed earlier to account for the chemical and isotopic compositions of the Karoo CFBs in southern Africa (Ellam and Cox, 1991; Ellam *et al.*, 1992). Still other workers have suggested that the low-titanium Norils'k area CFBs were derived exclusively from CLM contaminated by subducted sediments, although melting of the lithosphere may have been triggered by conductive heating from the Siberian plume when it impinged upon the base of the lithosphere (Lightfoot *et al.*, 1993).

The controversy regarding the origin of low-ε_{Nd}, low-titanium CFBs has also been intense for the ~130 Ma Paraná CFBs. The Paraná CFB province covers an area of at least 1.2×10^6 km^2; and consists of a central area of voluminous tholeiitic flood basalts surrounded by a smaller volume of alkalic intrusions and lavas (Peate, 1997). Amongst the flood basalts, low-titanium, low-ε_{Nd} basalts (the Gramado and Esmeralda basalts; Table 3) cover the southern half of the province, while high-titanium, higher-ε_{Nd} CFBs (e.g., Urubici basalts; Table 3) are present in the northern half (Peate, 1997). Some authors have suggested that the two magma types were generated in a common upwelling plume source. These

workers consider the high-titanium basalts to have been derived from deeper (within garnet stability field) and smaller degrees of partial melting than low-titanium basalts. The contrast in ε_{Nd} values between the two basalt types is interpreted as the result of differing amounts of crustal contamination (Fodor, 1987). Others have suggested that while evidence of minor crustal contamination exists for all the Paraná CFB (such as increasing $^{87}Sr/^{86}Sr$ with increasing Th/Ta ratios), the chemical and isotopic contrasts between the high- and low-titanium CFB are retained even in the least-contaminated rocks, suggesting that distinctly different parental magmas are required for the different CFBs (Peate and Hawkesworth, 1996). However, neither basalt type has chemical or isotopic compositions similar to basalts derived from the Tristan plume, which is probably responsible in some fashion for both CFB formation in the Paraná and Etendeka and for the opening of the southern Atlantic (Peate, 1997). If they are not plume derived, all the Paraná CFBs may be products of melting within the lithospheric mantle. If so, the compositional differences between the high- and low-titanium CFBs may represent regular north–south differences between the chemical and isotopic composition of the lithospheric mantle (Peate, 1997). Deriving such large volumes of magma from the lithospheric mantle is unlikely, if the mantle is initially cold and dry (Arndt and Christensen, 1992), but is theoretically possible if the mantle is initially wet and melts when conductively heated from below by an upwelling plume (Gallagher and Hawkesworth, 1992; Turner *et al.*, 1996b). However, mafic magmatism occurred again in southern Brazil during the Late Cretaceous, ~50 Myr after the emplacement of the Paraná CFB, possibly as a result of the impact of the Trinidade plume at the base of the mantle lithosphere. Gibson *et al.* (1999) argue that the alkaline magmatism produced at this time was derived from CLM that was metasomatically enriched in the Proterozoic. The preservation of such low-melting T-components in the lithospheric mantle, at least until the Late Cretaceous, suggests that the CLM beneath this region was not pervasively melted during the formation of the earlier Paraná CFB, as Turner *et al.* (1996b) had suggested. Clearly, the source of the Paraná basalts is still an open question.

The above discussion shows that the role of crustal contamination in the chemical and isotopic compositions of CFB remains an important issue. Some workers have suggested that this type of contamination can be most readily recognized through osmium-isotopic data, given the large osmium-isotopic contrast between mantle-derived magmas and the generally high $^{187}Os/^{188}Os$ of the continental crust (Chesley and Ruiz, 1998). Another promising approach to resolving the contamination issue is through the use of phenocryst oxygen-isotope data. A recent study of olivine, clinopyroxene, and plagioclase separates from Oligocene flood basalts in Yemen showed that these minerals have $\delta^{18}O$ values that deviate considerably from the values expected for either a lithospheric or sublithospheric mantle-derived magma undergoing fractional crystallization alone (Baker *et al.*, 2000). Olivine $\delta^{18}O$ values, for example, range from 5.1‰ to as high as 6.2‰. This increase correlates with a small but significant increase in whole-rock $^{87}Sr/^{86}Sr$, decrease in ε_{Nd}, and increased variability in whole-rock lead-isotopic compositions. These variations are clearly due to the assimilation of the high $^{87}Sr/^{86}Sr$ and $\delta^{18}O$, low ε_{Nd} Proterozoic basement of the Arabian Peninsula. Furthermore, because oxygen represents ~50% of a typical mantle or crustal rock (Taylor, 1968), the increase in magmatic $\delta^{18}O$ recorded in the phenocrysts requires a substantial amount of assimilation (up to ~25 wt.%, depending on the crustal $\delta^{18}O$). Addition of such large amounts of crust can shift the trace-element compositions of the basaltic magma dramatically, and could even produce a shift from the low-LILE/HFSE ratio typical of OIB and high-titanium CFB, to the high-LILE/HFSE ratio of low-titanium CFB and potassic alkali basalt (due to the high-LILE/HFSE ratios typical of intermediate to felsic composition crust; Baker *et al.*, 2000). While this is a provocative study, it remains to be demonstrated that phenocryst oxygen-isotope studies can provide similar insights into the importance of crustal assimilation in the generation of CFB worldwide. Granulite facies lower continental crust, for example, can have low, mantle-like $\delta^{18}O$ values (Valley, 1986). Lower crustal assimilation, therefore, need not always produce a significant increase in magmatic $\delta^{18}O$.

3.03.3.4 Case Example—Western United States

Although our understanding of the how and why of continental basaltic rock formation is incomplete, their generation clearly provides an opportunity to study the dynamic behavior of both the lithospheric and sublithospheric mantle beneath the continents. A good example of the extremes to which this approach can take is the study of Late Cenozoic basaltic magmatism in the Basin and Range and adjacent regions of western North America. Late Cenozoic

volcanism within the Basin and Range commenced at ~30 Ma after the subduction of oceanic lithosphere beneath the region had ceased and at the onset of extensional tectonism within the continental lithosphere (Stewart, 1998). There is general agreement that extensional tectonism was involved in some fashion in inducing the melting of sublithospheric and/or lithospheric mantle that led to the Late Cenozoic basaltic magmatism (Fitton *et al.*, 1991). As a result, spatial and temporal patterns in the chemical and isotopic compositions of the Late Cenozoic basalts should provide insights into changes in the sources of magmas within the Basin and Range and vicinity, information that, in turn, could be related to the mechanisms involved in lithospheric thinning. Because the volume of data available for these rocks is so large, it has become possible to attempt a detailed reconstruction of the Late Cenozoic history of the deep continental lithosphere in this region.

The first step in this reconstruction involves a detailed characterization of the chemical and isotopic variations of the basaltic rocks themselves. Both sodic and potassic basalts erupted in the Basin and Range in the Late Cenozoic. Sodic basalts with $\varepsilon_{Nd} > 0$ are found primarily within the Basin and Range proper. Generally, they have low-LIL/HFSE ratios, as well as low $^{87}Sr/^{86}Sr$, and lead-isotopic compositions that overlap those of Northern Hemisphere oceanic basalts (Kempton *et al.*, 1991). Sodic and potassic basalts with $\varepsilon_{Nd} < 0$, in contrast, are generally preserved within the western Great Basin (including the previously discussed Sierra Nevada basaltic rocks) and along the margins of the present-day Basin and Range (Kempton *et al.*, 1991). These basalts have high-LIL/HFSE ratios as well as generally high $^{87}Sr/^{86}Sr$, and lead-isotopic compositions characterized by high $^{207}Pb/^{204}Pb$ ratios at a given $^{206}Pb/^{204}Pb$ value relative to Northern Hemisphere oceanic basalts (Farmer *et al.*, 1989; Kempton *et al.*, 1991).

Because of the generally high LREE contents of all the western United States alkali basalts, their neodymium-isotopic compositions are likely to represent those of their mantle source regions. The high-ε_{Nd} (low-LIL/HFSE) and low-ε_{Nd} (high-LILE/HFSE) alkali basalts are typically, but not universally, interpreted as being derived from sublithospheric and slab-metasomatized lithospheric sources, respectively. There remains, however, the usual difficulty of defining whether mantle melting was provoked by active upwelling of a high-temperature mantle plume, or induced in passively upwelling upper mantle and/or in the overlying lithospheric mantle as a consequence of lithospheric extension. An important observation in this regard is the fact that the hafnium- and neodymium-isotopic compositions of alkali basalts plot on an array distinct from that for OIB. Beard and Johnson (1997) argue cogently that high-ε_{Nd} sodic basalts have combined neodymium- and hafnium-isotopic compositions that are consistent with their derivation not from a mantle plume but from a MORB upper mantle source that had undergone an ancient melt extraction in the spinel peridotite stability field (Beard and Johnson, 1997). Other workers have argued against a plume source based on the relatively low volume of Late Cenozoic magmatism produced in much of the Basin and Range (Bradshaw *et al.*, 1993).

As with the high-ε_{Nd} basalts, the low-ε_{Nd} basalts also plot off the OIB Hf–Nd array, which, along with their relatively radiogenic helium ($R_a \sim 6$; Reid and Graham, 1996; Dodson *et al.*, 1998), and lack of uranium-series disequilibria in the youngest basalts (Asmerom, 1999) argues for a lithospheric mantle source potentially metasomatized by subducted sediment just prior to stabilization of the Precambrian continental mantle lithosphere in this region (Fitton *et al.*, 1988). The sole dissenting voice is Wang *et al.* (2002), who suggest that high-iron content of low-ε_{Nd} basalts in southern Nevada requires a deep source for their parental magmas (Figure 4), below the geophysically defined base of the mantle lithosphere in this region. Melting at such depths requires a mantle potential temperature of at least 1,500 °C. These authors therefore suggest that the major-element composition of the basalts provides evidence for a mantle plume under the region.

Having more or less defined the sources of the Basin and Range basalts, the next step in extracting geodynamic information from the basalts is to determine what space–time patterns exist in the eruption of sublithosphere- versus lithosphere-derived basaltic rocks. In several areas within the Basin and Range, and particularly in the Rio Grande Rift, low-ε_{Nd} alkali basalts are followed by higher-ε_{Nd} basalts, including tholeiites (Perry *et al.*, 1987). A similar transition from low to high ε_{Nd} is found in alkali basalts of other regions experiencing large amounts of lithospheric extension, such as the Lake Mead extensional corridor in southern Nevada (DePaolo and Daley, 2000). In the Rio Grande Rift, this transition is interpreted as a direct response to lithospheric extension. Initial extension provoked melting in the lithosphere. This was followed by decompression melting of upwelling mantle directly beneath the rift axis (Perry *et al.*, 1987). The latter is manifested along the axis of the central Rio Grande Rift

by the eruption of sodic alkali basalts and tholeiitic basalts with ε_{Nd} values as high as $+5$ (Figure 18; Gibson *et al.*, 1993). The lithospheric mantle is preserved, however, along the rift flanks, where it undergoes conductive heating from the upwelling mantle and spawns low-volume, low-ε_{Nd} volcanism (Thompson and Gibson, 1994). This spatial and temporal pattern in the source of mafic magmatism along the rift is consistent with an overall "pure-shear" model for lithospheric extension, in which maximum crustal and mantle lithosphere extension are spatially coincident (Baldridge *et al.*, 1991).

It has also been suggested that extension within the Basin and Range may be accommodated in some regions by "simple shear," in which case the regions of maximum crustal and mantle lithosphere thinning are significantly displaced from one another (Wernicke *et al.*, 1988). In this case, the spatial–temporal pattern of basalt chemical and isotopic composition might be quite different from the pure-shear case, with basalt forming along the axis of maximum crustal thinning and undergoing a shift from lithosphere to sublithospheric source at a later time than those found in "off-axis" positions (Farmer *et al.*, 1989). Such a displacement could account for the contemporaneous eruption of low-ε_{Nd} basalt in southern Nevada and high-ε_{Nd} basalt in adjacent portions of Owens Valley to the west (Farmer *et al.*, 1989; DePaolo and Daley, 2000). Regardless of the exact interpretation involved, however, it is clear that regular spatial–temporal patterns do exist in the chemical and isotopic composition of Late Cenozoic basalts in the western United States, and integration of these observations into geodynamic models can provide important insights into the physical evolution of the deep continental lithosphere.

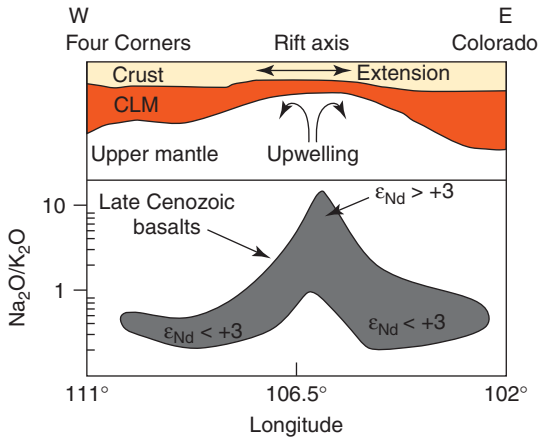

Figure 18 Cartoon depicting Late Cenozoic pure shear extension of central Rio Grande Rift, northern New Mexico, and range of Na_2O/K_2O for Late Cenozoic basaltic rocks (ultrapotassic, alkali, and tholeiitic composition) along a transect perpendicular to the rift axis. Thinning of mantle lithosphere beneath the rift axis triggers melting of upwelling asthenosphere, producing sodic composition, high-ε_{Nd} basaltic magmas, while along the rift flanks potassic magmas are generated via conductive heating within preserved, K-metasomatized portions of the pre-extension CLM. After Gibson *et al.* (1993).

3.03.4 INTRUSIVE EQUIVALENTS OF CONTINENTAL BASALTIC ROCKS

Because of the relatively high density of basaltic magmas ($\sim$2,600 kg m^{-3} at 10^{-4} GPa; Spera, 2000), it is likely that the bulk of mafic magmas produced beneath continents, particularly if anhydrous, will not reach the surface, but will instead crystallize at depth in the continental lithosphere. As a result, intrusive mafic magmatism may represent an important mechanism of continental growth (Johnson, 1991). One obvious manifestation of the intrusion and crystallization of mafic magmas in the continental crust is the presence of massive dike swarms, such as the Proterozoic McKenzie dike swarm in North America, which could represent the eroded underpinnings of pre-Mesozoic LIPs (Ernst and Buchan, 1997). Layered mafic intrusions also occur worldwide and range in age from Precambrian to Tertiary. These intrusions are significant both for establishing the crystallization history of mafic magmas and as an economic source of platinum-group metals (Cawthorn, 1999). Many of these intrusions may also be related to LIPs. The oft-studied Tertiary Skaergård intrusion in southeastern Greenland (McBirney, 2002) probably represents an intrusive equivalent of the basalts comprising portions of the North Atlantic igneous province, while the Precambrian Muskox intrusion in Canada could be related to the large magmatic event that produced the McKenzie dike swarm (Ernst and Buchan, 2001). Furthermore, in southern Africa, seismic evidence suggests that the magmatism that resulted in the Archean Bushveld layered mafic intrusion also produced a wholesale modification of the crustal and mantle lithosphere, including the introduction of iron into CLM during magmatism. This demonstrates the significance of mafic magmatism in modifying the volume and composition of the lithosphere (James *et al.*, 2001).

It has also been recognized that much of the lower continental crust worldwide is mafic in composition (Rudnick, 1992). This leads to the

question of whether the continents have been extensively underplated by mafic magmas, or whether mafic lower crust represents an original characteristic of the continents. Investigations of this issue have largely involved studies of mafic lower crustal xenoliths entrained in younger basalts or ultramafic magmas (Rudnick, 1992) and have included studies of both Phanerozoic and Precambrian lower crust.

Perhaps the best evidence for Phanerozoic underplating of the continental crust comes from mafic, granulite facies xenoliths entrained in Plio-Pleistocene basalts in north Queensland, Australia (Rudnick *et al.*, 1986). Here, xenoliths show a negative correlation between incompatible element content and mg#. Furthermore, the xenoliths' ε_{Nd} decreases, and $^{87}Sr/^{86}Sr$ increases, with decreasing mg#. Both the trace-element and isotopic data are consistent with the notion that the xenoliths represent cumulates from Cenozoic basaltic magmas that intruded the lower crust and underwent concomitant fractional crystallization and crustal assimilation. This example demonstrates that underplating of mafic magmas can occur, but because xenoliths represent a nonrepresentative and incomplete sampling of the lower crust, it is not clear whether this underplating represents a significant contribution to the overall mass of the continental crust in this region.

Xenoliths of Precambrian mafic lower crust have been studied in various locations worldwide, such as the western United States, northern Europe, and southern Africa (Selverstone *et al.*, 1999; Carlson *et al.*, 2000; Kempton *et al.*, 2001). Extracting unambiguous age and compositional information regarding the lower crust from these rocks is difficult, because they were extracted from continental crust that has potentially undergone multiple episodes of high-pressure ± high-temperature metamorphism, partial melting, and metasomatism. As a result, it is not easy to decide whether these rocks represent mafic lithologies that were present in the lower crust at the time of crustal stabilization, or whether they represent subsequently underplated material. Kempton *et al.* (2001) argue that plagioclase-bearing garnet granulites entrained in Devonian lamprophyres from the Baltic Shield represent solidified tholeiitic melts. These authors suggest that the xenoliths represent portions of 2.4–2.5-Gyr-old lower crust emplaced during the development of a large, plume-related Late Archean igneous province. Other authors have suggested that mantle plumes, perhaps related to episodes of mantle overturn, can produce significant crustal growth (Stein and Hoffman, 1994). The chemical composition of lower crustal xenoliths, however, is not always consistent with an origin via underplating by plume-related magmas. Many xenolith suites, including those from the Colorado Plateau and the southern margin of the Archean Wyoming craton in the western United States, have low nickel contents and high La/Nb ratios, as expected for arc-related magmas, or magmas that had interacted with the continental crust (Selverstone *et al.*, 1999). These rocks apparently represent mafic lower crust that formed at or near the time of crustal stabilization by subduction-related magmas. There is the possibility, then, that mafic lower crust of two general flavors exist, one produced by subduction-related processes at or near the time of crust formation, and a second with low La/Nb ratios and higher nickel contents produced during plume-related episodes of mafic magma underplating (Condie, 1999). It remains for future studies to assess the validity of this suggestion, and to determine the relative proportion of mafic lower crust formed by subduction- and plume-related processes.

3.03.5 CONCLUDING REMARKS

Considerable progress has been made during the past few decades in identifying the processes involved in the production of continental basaltic magmatism, but some fundamental questions remain. For example, if the continental mantle lithosphere is a source of continental magmatism, how critical are mafic lithologies in CLM to the production of such magmas and in controlling their chemical composition? Do reactions between ultramafic lithologies and partial melts of mafic lithologies produce the immediate sources of some continental basalts (Carlson and Nowell, 2001)? Is metasomatism of the CLM by fluids/melt derived from the sublithospheric mantle a necessary immediate precursor to the production of not only kimberlites but also both sodic and potassic continental alkali basalts? Does pervasively metasomatized mantle exist at the base, or some other depth, within the CLM, and if so, what are its physical properties? Under what conditions can hydrated CLM be preserved, and under what circumstances does such mantle get involved in continental magmatism?

These questions do not just involve a few details in an overall known picture of continental basaltic magma formation. They represent fundamental issues regarding the generation of these magmas. The basic issue remains whether the geochemistry of continental basaltic rocks can distinguish rocks derived

primarily from melting of the lithospheric mantle or from those derived primarily from the sublithospheric mantle. A complication discovered by recent studies is the increasing recognition that the lithospheric mantle is dynamic, can change thickness through time, and contains components of varying chemical and isotopic composition that were introduced at different times during the history of a given segment of CLM. If a better understanding of the sources of continental basaltic rocks can be achieved, these rocks will provide additional insights into the evolution of the deep continental lithosphere.

ACKNOWLEDGMENTS

This chapter benefited greatly from comments by Dawnika Blatter and from the patient editorial handling by Roberta Rudnick.

REFERENCES

Anderson D. L. (1995) Lithosphere, asthenosphere, and perisphere. *Rev. Geophys.* **33**, 125–149.

Arndt N. T. and Christensen U. (1992) The role of lithospheric mantle in continental flood volcanism: thermal and geochemical constraints. *J. Geophys. Res.* **97**, 10967–10981.

Arndt N. T., Czamanske G. K., Wooden J. L., and Fedorenko V. A. (1993) Mantle and crustal contributions to continental flood volcanism. *Tectonophysics* **223**, 39–52.

Arndt N. T., Ginibre C., Chauvel C., Albarede F., Cheadle M., Herzberg C., Jenner G., and Lahaye Y. (1998) Were komatiites wet? *Geology* **26**, 739–742.

Asmerom Y. (1999) Th–U fractionation and mantle structure. *Earth Planet. Sci. Lett.* **166**, 163–175.

Baker J. A., MacPherson C. G., Menzies M. A., Thirlwall M. F., Al-Kadasi M., and Mattey D. P. (2000) Resolving crustal and mantle contributions to continental flood volcanism, Yemen; constraints from mineral oxygen isotope data. *J. Petrol.* **41**, 1805–1820.

Baker J. A., Menzies M. A., Thirlwall M. F., and MacPherson C. G. (1997) Petrogenesis of Quaternary intraplate volcanism, Sana'a, Yemen: implications for plume–lithosphere interaction and polybaric melt hybridization. *J. Petrol.* **38**, 1359–1390.

Baker M. B. and Stolper E. M. (1994) Determining the composition of high-pressure mantle melts using diamond aggregates. *Geochim. Cosmochim. Acta* **58**, 2811–2827.

Baldridge W. S., Keller G. R., Haak V., Wendlandt E., Jiracek G. R., and Olsen K. H. (1995) The Rio Grande Rift. In *Continental Rifts: Evolution, Structure, Tectonics, Developments in Geotectonics* (ed. K. H. Olsen). Elsevier, Amsterdam, vol. 25, pp. 233–275.

Baldridge W. S., Perry F. V., Vaniman D. T., Nealey L. D., Leavy B. D., Laughlin A. W., Kyle P., Bartov Y., Steinitz G., and Gladney E. S. (1991) Middle to late Cenozoic magmatism of the southeastern Colorado Plateau and central Rio Grande Rift (New Mexico and Arizona, USA): a model for continental rifting. *Tectonophysics* **197**, 327–354.

Barfod D. N., Ballentine C. J., Halliday A. N., and Fitton J. G. (1999) Noble gases in the Cameroon line and the He, Ne, and Ar isotopic compositions of high μ (HIMU) mantle. *J. Geophys. Res.* **104**, 29509–29527.

Barrell J. (1914) The strength of the Earth's crust. *J. Geol.* **22**, 425–433.

Basu A. R., Hannigan R. E., and Jacobsen S. B. (1998) Melting of the Siberian mantle plume. *Geophys. Res. Let.* **25**, 2209–2212.

Basu A. R., Poreda R. J., Renne P. R., Teichmann F., Vasiliev Y. R., Sobolev N. V., and Turrin B. D. (1995) High-3He plume origin and temporal–spatial evolution of the Siberian flood basalts. *Science* **269**, 822–825.

Basu A. R., Renne P. R., Dasgupta D. K., Teichmann F., and Poreda R. J. (1993) Early and late alkali igneous pulses and a high-(super 3) He plume origin for the Deccan flood basalts. *Science* **261**, 902–906.

Beard B. L. and Johnson C. M. (1993) Hf isotope composition of late Cenozoic basaltic rocks from northwestern Colorado, USA: new constraints on mantle enrichment processes. *Earth Planet. Sci. Lett.* **119**, 495–509.

Beard B. L. and Johnson C. M. (1997) Hafnium isotope evidence for the origin of Cenozoic basaltic lavas from the southwestern United States. *J. Geophys. Res.* **102**, 20149–20178.

Beattie P. (1993) Uranium–thorium disequilibria and partitioning on melting of garnet peridotite. *Nature* **363**, 63–65.

Bohrson W. A. and Spera F. J. (2001) Energy-constrained open-system magmatic processes. I: General model and energy-constrained assimilation and fractional crystallization (EC-AFC) formulation. *J. Petrol.* **42**, 1019–1041.

Bradshaw T. K., Hawkesworth C. J., and Gallagher K. (1993) Basaltic volcanism in the southern Basin and Range: no role for a mantle plume. *Earth Planet. Sci. Lett.* **116**, 45–62.

Carlson R. W., Boyd F. R., Shirey S. B., Janney P. E., Grove T. L., Bowring S. A., Schmitz M. D., Dann J. C., Bell D. R., Gurney J. J., Richardson S. H., Tredoux M., and Menzies A. H. (2000) Continental growth, preservation, and modification in southern Africa. *GSA Today* **10**, 1–7.

Carlson R. W. and Nowell G. M. (2001) Olivine-poor sources for mantle-derived magmas: Os and Hf isotopic evidence from potassic magmas of the Colorado Plateau. *Geochem. Geophys. Geosyst.* **2**, 200GC000128.

Cawthorn R. G. (1999) Platinum-group element mineralization in the Bushveld Complex: a critical reassessment of geochemical models. *S. Afr. J. Geol.* **102**, 268–281.

Chesley J. T. and Ruiz J. (1998) Crust–mantle interaction in large igneous provinces: implications from the Re–Os isotope systematics of the Columbia River flood basalts. *Earth Planet. Sci. Lett.* **154**, 1–11.

Chesley J., Ruiz J., Righter K., Ferrari L., and Gomez-Tuena A. (2002) Source contamination versus assimilation: an example from the Trans-Mexican Volcanic Arc. *Earth Planet. Sci. Lett.* **195**, 211–221.

Chung S. L. (1999) Trace element and isotope characteristics of Cenozoic basalts around the Tanlu fault with implications for the eastern plate boundary between north and south China. *J. Geol.* **107**, 301–312.

Chung S. L. and Jahn B. M. (1995) Plume–lithosphere interaction in generation of the Emeishan flood basalts at the Permian–Triassic boundary. *Geology* **23**, 889–892.

Chung S. L., Jahn B. M., Chen S. J., Lee T., and Chen C. H. (1995) Miocene basalts in northwestern Taiwan: evidence for EM-type mantle sources in the continental lithosphere. *Geochim. Cosmochim. Acta* **59**, 549–555.

Chung S. L., Lo C. H., Lee T. Y., Zhang Y., Xie Y., Xinhua L., Wang K. L., and Wan P. L. (1998) Diachronous uplift of the Tibetan plateau starting 40 Myr ago. *Nature* **394**, 769–773.

Chung S. L., Wang K. L., Crawford A. J., Kamenetsky V. S., Chen C. H., Lan C. Y., and Chen C. H. (2001) High-Mg potassic rocks from Taiwan: implications for the genesis of orogenic potassic lavas. *Lithos* **59**, 153–170.

Class C., Altherr F. V., Eberz C., and McCulloch M. T. (1994) Geochemistry of Pliocene to Quaternary alkali basalts from the Huri Hills, northern Kenya. *Chem. Geol.* **113**, 1–22.

Class C. and Goldstein S. L. (1997) Plume–lithosphere interactions in the ocean basins: constraints from the source mineralogy. *Earth Planet. Sci. Lett.* **150**, 245–260.

Coffin M. F. and Eldholm O. (1994) Large igneous provinces: crustal structure, dimension, and external consequences. *Rev. Geophys.* **32**, 1–36.

Condie K. C. (1993) Chemical composition and evolution of the upper continental crust; contrasting results from surface samples and shales. *Chem. Geol.* **104**, 1–37.

Condie K. C. (1999) Mafic crustal xenoliths and the origin of the lower continental crust. *Lithos* **46**, 95–101.

Connor, C. B. and Conway, F. M. (2000) Basaltic volcanic fields. In *Encylopedia of Volcanoes* (ed. H. Sigurdsson). Academic Press, San Diego, pp. 331–343.

Conticelli S., Francalianci L., Manetti P., Cioni R., and Sbrana A. (1997) Petrology and geochemistry of the ultrapotassic rocks from the Sabatini volcanic district, central Italy: the role of evolutionary process in the genesis of variably enriched alkaline magmas. *J. Volcanol. Geotherm. Res.* **7–5**, 107–136.

Cordery M. J., Davies G. F., and Campbell I. H. (1997) Genesis of flood basalts from eclogite-bearing mantle plumes. *J. Geophys. Res.* **102**, 20179–20197.

Courtillot V., Besse J., Vandamme D., Montigny R., Jaeger J. J., and Cappeta H. (1999) Deccan flood basalts at the Cretacous/Tertiary boundary? *Earth Planet Sci. Lett.* **80**, 361–374.

Dalpé C. and Baker D. R. (2000) Experimental investigation of large-ion-lithophile-element-, high-field-strength-element and rare-earth-element-partitioning between calcic amphibole and basaltic melt: the effects of pressure and oxygen fugacity. *Contrib. Mineral. Petrol.* **140**, 233–250.

Dawson J. B. (1967) A review of the geology of kimberlites. In *Ultramafic and Related Rocks* (ed. P. J. Wyllie). Wiley, New York, pp. 241–251.

DePaolo D. J. and Daley E. E. (2000) Neodymium isotopes in basalts of the southwest basin and range and lithospheric thinning during continental extension. *Chem. Geol.* **169**, 157–185.

Dobosi G., Downes H., Mattey D., and Embey-Isztin A. (1998) Oxygen isotope ratios of phenocrysts from alkali basalts of the Pannonian basin: evidence for an O-isotopically homgeneous upper mantle beneath a subduction-influenced area. *Lithos* **42**, 213–223.

Dodson A., DePaolo D. J., and Kennedy B. M. (1998) Helium isotopes in lithospheric mantle: evidence from Tertiary basalts of the western USA. *Geochim. Cosmochim. Acta* **62**, 3775–3787.

Dungan M. A., Lindstrom M. M., McMillan N. J., Moorbath S., Hoefs J., and Haskin L. A. (1986) Open system magmatic evolution of the Taos Plateau volcanic field, northern New Mexico. 1: The petrology and geochemistry of the Servilleta Basalt. *J. Geophys. Res.* **91**, 5999–6028.

Edwards D., Rock N. M. S., Taylor W. R., Griffin W. L., and Ramsay R. R. (1992) Mineralogy and petrology of the Aries diamondiferous kimberlite pipe, central Kimberley Block, western Australia. *J. Petrol.* **33**, 1157–1191.

Eiler J. M., Farley K. A., Valley J. W., Hauri E. H., Harmon C., Hart S. R., and Stolper E. M. (1997) Oxygen isotope variations in ocean island basalt phenocrysts. *Geochim. Cosmochim. Acta* **61**, 2281–2293.

Elkins L. T. and Hager B. H. (2000) Melt intrusion as a trigger for lithospheric foundering and the eruption of the Siberian flood basalts. *Geophys. Res. Lett.* **27**, 3937–3940.

Ellam R. M., Carlson R. W., and Shirey S. B. (1992) Evidence from Re–Os isotopes for plume–lithosphere mixing in Karoo flood basalt genesis. *Nature* **359**, 718–721.

Ellam R. M. and Cox K. G. (1991) An interpretation of Karoo picrite basalts in terms of interaction between asthenospheric magmas and the mantle lithosphere. *Earth Planet Sci. Lett.* **105**, 330–342.

Ernst, R. E. and Buchan, K. L. (1997) Giant radiating dyke swarms: their use in identifying pre-Mesozoic large igneous provinces and mantle plumes. In *Large Igneous Provinces* (eds. J. J. Mahoney and M. F. Coffin), Geophysical Monograph 100. American Geophysical Union, Washington, DC, pp. 297–333.

Ernst, R. E. and Buchan, K. L. (2001) Large mafic magmatic events through time and links to mantle-plume heads. In *Mantle Plumes: Their Identification Through Time* (eds. R. E. Ernst and K. L. Buchan), Geological Society of America Special Paper 252. Geological Society of America, Boulder, CO, pp. 483–575.

Farmer G. L., Glazner A. F., and Manley C. R. (2002) Did lithospheric delamination trigger late Cenozoic potassic volcanism in the southern Sierra Nevada, California? *Geol. Soc. Am. Bull.* **114**, 754–768.

Farmer G. L., Glazner A. F., Wilshire H. G., Wooden J. L., Pickthorn W. J., and Katz M. (1995) Origin of late Cenozoic basalts at the Cima volcanic field, Mojave Desert, California. *J. Geophys. Res.* **100**, 8399–8415.

Farmer G. L., Perry F. V., Semken S., Crowe B., Curtis D., and DePaolo D. J. (1989) Isotopic evidence on the structure and origin of subcontinental lithospheric mantle in southern Nevada. *J. Geophys. Res.* **94**, 7885–7898.

Feldstein S. N. and Lange R. A. (1999) Pliocene potassic magmas from the Kings River region, Sierra Nevada, California: evidence for melting of a subduction-modified mantle. *J. Petrol.* **40**, 1301–1320.

Fitton J. G., Dodie J., and Leeman W. P. (1991) Basic magmatism associated with late Cenozoic extension in the western United States: compositional variations in space and time. *J. Geophys. Res.* **96**, 13693–13711.

Fitton J. G. and Dunlop H. M. (1985) The Cameroon Line, West Africa, and its bearing on the origin of oceanic and continental alkali basalt. *Earth Planet. Sci. Lett.* **72**, 23–38.

Fitton J. G., James D., Kempton P. D., Ormerod D. S., and Leeman W. P. (1988) The role of lithospheric mantle in the generation of late Cenozoic basic magmas in the western United States. *J. Petrol.* (Spec. Lithosphere Issue), 331–349.

Fodor R. V. (1987) Low- and high-TiO_2 flood basalts of southern Brazil: origin from picritic parentage and a common mantle source. *Earth Planet. Sci. Lett.* **84**, 423–430.

Foley S. (1992) Vein-plus-wall-rock melting mechanisms in the lithosphere and the origin of potassic alkaline magmas. *Lithos* **28**, 435–453.

Franz G., Steiner G., Volker F., Pudlo D., and Hammerschmidt K. (1999) Plume-related alkaline magmatism in central Africa—the Meidob Hills (W. Sudan). *Chem. Geol.* **157**, 27–47.

Frey F. A. and Green D. H. (1974) Mineralogy, geochemistry and origin of lherzolite inclusions in Victorian basanites. *Geochim. Cosmochim. Acta* **38**, 1023–1059.

Furman T. (1995) Melting of metasomatized subcontinental lithosphere: undersaturated mafic lavas from Rungwe, Tanzania. *Contrib. Mineral. Petrol.* **122**, 97–115.

Furman T. and Graham D. (1999) Erosion of lithospheric mantle beneath the East African Rift system: geochemical evidence from the Kivu volcanic province. *Lithos* **48**, 237–262.

Gallagher K. and Hawkesworth C. (1992) Dehydration melting and the generation of continental flood basalts. *Nature* **258**, 57–59.

Gibson S. A. (2002) Major element heterogeneity in Archean to Recent mantle plume starting-heads. *Earth Planet. Sci. Lett.* **195**, 59–74.

Gibson S. A., Thompson R. N., and Dickin A. P. (2000) Ferropicrites: geochemical evidence for Fe-rich streaks in upwelling mantle plumes. *Earth Planet. Sci. Lett.* **173**, 355–374.

Gibson S. A., Thompson R. N., Leat P. T., Morrison M. A., Hendry G. L., Dickin A. P., and Mitchell J. G. (1993) Ultrapotassic magmas along the flanks of the Oligo-Miocene Rio Grande Rift, USA—monitors of the zone of lithospheric mantle extension and thinning beneath a continental rift. *J. Petrol.* **34**, 187–228.

Gibson S. A., Thompson R. N., Leonardos O. H., Dickin A. P., and Mitchell J. G. (1999) The limited extent of plume–lithosphere interactions during continental flood-basalt genesis: geochemical evidence from Cretaceous magmatism in southern Brazil. *Contrib. Mineral. Petrol.* **137**, 147–169.

Girnis A. V., Brey G. P., and Ryabchikov I. D. (1995) Origin of Group 1A kimberlites: fluid-saturated melting experiments at 45–55 kbar. *Earth Planet. Sci. Lett.* **134**, 283–296.

Glazner A. F. and Farmer G. L. (1992) Production of isotopic variability in continental basalts by cryptic crustal contamination. *Science* **255**, 72–74.

Griffin W. L., O'Reilly S. Y., and Ryan C. G. (1999) The composition and origin of sub-continental lithospheric mantle. In *Mantle Petrology: Field Observations and High Pressure Experimentation* (eds. Y. Fei, C. M. Bertka, and B. O. Mysen), Special Publication no. 6. The Geochemical Society, Houston, pp. 13–45.

Grove T. L. (2000) Origin of magmas. In *Encyclopedia of Volcanoes* (ed. H. Sigurdsson). Academic Press, San Diego, pp. 133–147.

Hames W. E., Renne P. R., and Ruppel C. (2000) New evidence for geologically instantaneous emplacement of earliest Jurassic Central Atlantic magmatic province basalts on the North American margin. *Geology* **28**, 859–862.

Hanson G. N. (1989) An approach to trace element modeling using a simple igneous system as an example. In *Geochemistry and Mineralogy of Rare Earth Elements* (eds. B. R. Lipin and G. A. McKay). *Rev. Mineral.*, Mineralogical Society of America, Washington, DC, vol. 21, pp. 79–89.

Harry D. L. and Leeman W. P. (1995) Partial melting of melt metasomatized subcontinental mantle and the magma source potential of the lower lithosphere. *J. Geophys. Res.* **100**, 10255–10269.

Hart S. R. (1984) A large-scale isotope anomaly in the Southern Hemisphere mantle. *Nature* **309**, 753–757.

Hart W. K., Carlson R. W., and Shirey S. B. (1997) Radiogenic Os in primitive basalts from the northwestern USA: implications for petrogenesis. *Earth Planet. Sci. Lett.* **150**, 103–116.

Heaman L. M. and Kjarsgaard B. A. (2000) Timing of eastern North American kimberlite magmatism: continental extension of the Great Meteor hotspot track? *Earth Planet. Sci. Lett.* **178**, 253–268.

Hergt J. M., Peate D. W., and Hawkesworth C. J. (1991) The petrogenesis of Mesozoic Gondwana low-Ti flood basalts. *Earth Planet. Sci. Lett.* **105**, 134–148.

Herzberg C. and O'Hara M. J. (1998) Phase equilibrium constraints on the origin of basalts, picrites, and komatiites. *Earth Sci. Rev.* **44**, 39–79.

Hirose K. and Kushiro I. (1993) Partial melting of dry peridotites at high pressures: determinations of compositions of melts segregated from peridotite using aggregates of diamond. *Earth Planet. Sci. Lett.* **114**, 477–489.

Hoang N. and Flower M. (1998) Petrogenesis of Cenozoic basalts from Vietnam: implications for origins of a "diffuse igneous province." *J. Petrol.* **39**, 369–395.

Hofmann A. W. (1997) Mantle geochemistry: the message from oceanic magmatism. *Nature* **385**, 219–229.

Hole M. J. (1988) Post-subduction alkaline volcanism along the Antarctic Peninsula. *J. Geol. Soc. London* **145**, 985–998.

Hole M. J., Rogers G., Saunders A. D., and Storey M. (1991) Relation between alkalic volcanism and slab-window formation. *Geology* **19**, 657–660.

Hooper P. R. (2000) Flood basalt provinces. In *Encyclopedia of Volcanoes* (ed. H. Sigurdsson). Academic Press, San Diego, pp. 345–359.

Hooper P. R. and Hawkesworth C. J. (1993) Isotopic and geochemical constraints on the origin and evolution of the Columbia River Basalt. *J. Petrol.* **34**, 1203–1246.

Horan M. F., Walker R. J., Fedorenko V. A., and Czamanske G. K. (1995) Osmium and neodymium isotopic constraints on the temporal and spatial evolution of Siberian flood basalt sources. *Geochim. Cosmochim. Acta* **59**, 5159–5168.

Hornig I. (1993) High-Ti and low-Ti tholeiites in the Jurassic Ferrar Group, Antarctica. *Geol. Jahr. Reihe E: Geophysik* **47**, 335–369.

Iddings J. P. (1892) The origin of igneous rocks. *Bull. Phil. Soc. Wash.* **12**, 89–213.

Irvine T. N. and Baragar W. R. A. (1971) A guide to the chemical classification of the common volcanic rocks. *Can. J. Earth Sci.* **8**, 523–548.

James D. E., Fouch M. J., VanDecar J. C., and van der Lee S. (2001) Tectospheric structure beneath southern Africa. *Geophys. Res. Lett.* **28**, 2485–2488.

Johnson C. M. (1991) Large-scale crust formation and lithosphere modification beneath Middle to Late Cenozoic calderas and volcanic fields, western North America. *J. Geophys. Res.* **96**, 13485–13507.

Johnson R. W., Knutson J., and Taylor S. R. (1989) *Intraplate Volcanism in Eastern Australia and New Zealand*. Cambridge University Press, Cambridge.

Jordan T. H. (1978) Composition and development of continental tectosphere. *Nature* **274**, 544–548.

Jordan T. H. (1988). Structure and formation of the continental tectosphere. *J. Petrol.* (Spec. Lithosphere Issue), 11–37.

Jung S. and Hoernes S. (2000) The major- and trace-element and isotope (Sr, Nd, O) geochemistry of Cenozoic alkaline rift-type volcanic rocks from the Rhon area (central Germany): petrology, mantle source characteristics and implications for asthenosphere–lithosphere interactions. *J. Volcan. Geotherm. Res.* **99**, 27–53.

Kelemen P. B., Hart S. R., and Bernstein S. (1998) Silica enrichment in the continental upper mantle via melt/rock reaction. *Earth Planet. Sci. Lett.* **164**, 387–406.

Kempton P. D., Downes H., Neymark L. A., Wartho J. A., Zartman R. E., and Sharkov E. V. (2001) Garnet granulite xenoliths from the northern Baltic Shield—the underplated lower crust of a Palaeoproteroic large igneous province. *J. Petrol.* **42**, 731–763.

Kempton P. D., Fitton J. G., Hawkesworth C. J., and Ormerod D. S. (1991) Isotopic and trace element constraints on the composition and evolution of the lithosphere beneath the southwestern United States. *J. Geophys. Res.* **96**, 13713–13735.

King S. D. and Anderson D. L. (1998) Edge-driven convection. *Earth Planet. Sci. Lett.* **160**, 289–296.

Korenaga J. and Kelemen P. B. (2000) Major element heterogeneity in the mantle source of the North Atlantic igneous province. *Earth Planet. Sci. Lett.* **184**, 251–268.

Kushiro I. (2001) Partial melting experiments on peridotite and origin of mid-ocean ridge basalt. *Ann. Rev. Earth Planet. Sci.* **29**, 71–107.

Landwehr D., Blundy J., Chamorro-Perez E., Hill E., and Wood B. (2001) U-series disequilibria generated by partial melting of spinel lherzolite. *Earth Planet. Sci. Lett.* **188**, 329–348.

Lange R. A. (2002) Constraints on the preeruptive volatile concentrations in the Columbia River basalts. *Geology* **30**, 179–182.

Langmuir C. H., Klein E. M., Plank T. (1992) Petrological systematics of mid-ocean ridge basalts: constraints on melt generation beneath ocean ridges. In *Mantle Flow and Melt Generation at Mid-Ocean Ridges* (eds. J. P. Morgan, D. K. Blackman, and J. M. Sinton), Geophysical Monograph 71. American Geophysical Union, Washington, DC, pp. 183–280.

Lassiter J. C. and DePaolo D. J. (1997) Plume/lithosphere interaction in the generation of continental and oceanic flood basalts: chemical and isotopic constraints. In *Large Igneous Provinces* (eds. J. J. Mahoney and M. F. Coffin), Geophysical Monograph 100. American Geophysical Union, Washington, DC, pp. 335–355.

Le Bas M. J. (2000) IUGS reclassification of the high-Mg and picritic volcanic rocks. *J. Petrol.* **41**, 1467–1470.

le Roex A. P. (1986) Geochemical correlation between southern African kimberlites and South Atlantic hotspots. *Nature* **324**, 243–245.

le Roex A. P., Spath A., and Zartman R. E. (2001) Lithospheric thickness beneath the southern Kenya Rift: implications from basalt geochemistry. *Contrib. Mineral. Petrol.* **142**, 89–106.

Lee C. T., Yin Q., Rudnick R., Chesley J. T., and Jacobsen S. B. (2000) Osmium isotopic evidence for Mesozoic removal of lithospheric mantle beneath the Sierra Nevada, California. *Science* **289**, 1912–1916.

Lee C. T., Yin Q., Rudnick R., and Jacobsen S. B. (2001) Preservation of ancient and fertile lithospheric mantle beneath the southwestern United States. *Nature* **411**, 69–72.

Leeman W. P. and Harry D. L. (1993) A binary source model for extension-related magmatism in the Great Basin, western North America. *Science* **262**, 1550–1554.

Lester A. P., Larson E. E., Farmer G. L., Stern C. R., and Funk J. A. (2001) Neoproterozoic kimberlite emplacement in the Front Range, Colorado. *Rocky Mount. Geol.* **36**, 1–12.

Lightfoot P. C., Hawkesworth C. J., Devey C. W., Rogers N. W., and Van Calsteren P. W. C. (1990) Source and differentiation of Deccan Trap lavas: implications of geochemical and mineral chemical variations. *J. Petrol.* **31**, 1165–1200.

Lightfoot P. C., Hawkesworth C. J., Hergt J., Naldrett A. J., Gorbachev N. S., Fedorenko V. A., and Doherty W. (1993) Remobilization of continental lithosphere by a mantle plume: major-trace-element, and Sr-, Nd- and Pb-isotopic evidence from picritic and tholeiitic lavas of the Norils'k District, Siberian Trap, Russia. *Contrib. Mineral. Petrol.* **114**, 171–188.

Mahoney, J. J. (1988). Deccan Traps. In *Continental Flood Basalts* (ed. J. D. Macdougall). Kluwer Academic, Dordrecht, 341pp.

Mahotkin I. L., Gibson S. A., Thompson R. N., Zhuravlev D. Z., and Zherdev P. U. (2000) Late Devonian diamondiferous kimberlite and alkaline picrite (protokimberlite) magmatism in the Arkhangelsk region, NW Russia. *J. Petrol.* **41**, 201–227.

Marzoli A., Piccirillo E. M., Renne P. R., Bellieni G., Iacumin M., Nyobe J. B., and Tongwa A. T. (2000) The Cameroon Volcanic Line revisted: petrogenesis of continental basaltic magmas from lithospheric and asthenospheric mantle sources. *J. Petrol.* **41**, 87–109.

McBirney A. R. (2002) The Skaergaard layered series: Part VI. Excluded trace elements. *J. Petrol.* **43**, 535–556.

McBride J. S., Lambert D. D., Nicholls I. A., and Price R. C. (2001) Osmium isotopic evidence for crust–mantle interaction in the genesis of continental intraplate basalts from the Newer Volcanic Province southeastern Australia. *J. Petrol.* **42**, 1197–1218.

McCulloch M. T. and Gamble J. A. (1991) Geochemical and geodynamical constraints on subduction zone magmatism. *Earth Planet. Sci. Lett.* **102**, 358–374.

McDonough W. F., McCulloch M. T., and Sun S. S. (1985) Isotopic and geochemical systematics in Tertiary–Recent basalts from southeastern Australia and implications for the evolution of the subcontinental mantle. *Geochim. Cosmochim. Acta* **49**, 2051–2067.

McDonough W. F., Sun S. S., Ringwood A. E., Jagoutz E., and Hofmann A. W. (1992) Potassium, rubidium, and cesium in the Earth and Moon and the evolution of the mantle of the Earth. *Geochim. Cosmochim. Acta* **56**, 1001–1012.

McKenzie D. (1989) Some remarks on the movement of small melt fractions in the mantle. *Earth Planet. Sci. Lett.* **95**, 53–72.

McKenzie D. and Bickle M. J. (1988) The volume and composition of melt generated by extension of the lithosphere. *J. Petrol.* **29**, 625–679.

McKenzie D. and O'Nions R. K. (1991) Partial melt distributions from inverstion of rare earth element concentrations. *J. Petrol.* **32**, 1021–1091.

Menzies M. A., Baker J. A., Chazo G., Al'Kadasi M. (1997) Evolution of the Red Sea volcanic margin, western Yemen. In *Large Igneous Provinces* (eds. J. J. Mahoney and M. F. Coffin), Geophysical Monograph 100. American Geophysical Union, Washington, DC, pp. 29–44.

Miller C., Schuster R., Klotzli U., Frank W., and Purtscheller F. (1999) Post-collisional potassic and ultrapotassic magmatism in SW Tibet: geochemical and Sr–Nd–Pb–O isotopic constraints for mantle source characteristics and petrogenesis. *J. Petrol.* **40**, 1399–1424.

Mitchell R. H. (1995) *Kimberlites, Orangeites, and Related Rocks*. Plenum, New York.

Mohr P. (1992) Nature of the crust beneath magmatically active continental rifts. *Tectonophysics* **213**, 269–284.

Moreira M. and Kurz M. D. (2001) Subducted oceanic lithosphere and the origin of the "high m" basalt helium signature. *Earth Planet. Sci. Lett.* **189**, 49–57.

Morgan W. J. (1971) Convection plumes in the lower mantle. *Nature* **230**, 42–43.

Nelson D. R. (1992) Isotopic characteristics of potassic rocks: evidence for the involvement of subducted sediments in magma genesis. *Lithos* **28**, 403–420.

Oyarzun R., Doblas M., Lopez-Ruiz J., and Cebria J. M. (1997) Opening of the central Atlantic and asymmetric mantle upwelling phenomena: implications for long-lived magmatism in western North Africa and Europe. *Geology* **25**, 727–730.

Parman S. W., Grove T. L., and Dann J. C. (2001) The production of Barbeton komatiites in an Archean subduction zone. *Geophys. Res. Lett.* **28**, 2513–2516.

Paslick C., Halliday A., James D., and Dawson J. B. (1995) Enrichment of the continental lithosphere by OIB melts: isotopic evidence from the volcanic province of northern Tanzania. *Earth Planet. Sci. Lett.* **130**, 109–126.

Pearce J. A. and Peate D. W. (1995) Tectonic implications of the composition of volcanic arc magmas. *Ann. Rev. Earth Planet. Sci.* **23**, 252–285.

Pearson D. G. (1999) Evolution of cratonic lithospheric mantle: an isotopic perspective. In *Mantle Petrology: Field Observations and High-pressure Experimentation* (eds. Y. Fei, C. M. Bertka, and B. O. Mysen). The Geochemical Society, Houston, vol. 6, pp. 57–78.

Peate D. W. (1997). The Paraná-Etendeka Province. In *Large Igneous Provinces* (eds. J. J. Mahoney and M. F. Coffin), Geophysical Monograph 100. American Geophysical Union, Washington, DC, pp. 217–245.

Peate D. W. and Hawkesworth C. J. (1996) Lithospheric to asthenospheric transition in low-Ti flood basalts from southern Paraná, Brazil. *Chem. Geol.* **127**, 1–24.

Peccerillo A. (1999) Multiple mantle metasomatism in central-southern Italy: geochemical effects, timing and geodynamic implications. *Geology* **27**, 315–318.

Perry F. V., Baldridge W. S., and DePaolo D. J. (1987) Role of asthenosphere and lithosphere in the genesis of late Cenozoic basaltic rocks from the Rio Grande Rift and adjacent regions of the southwestern United States. *J. Geophys. Res.* **92**, 9193–9213.

Pertermann M. and Hirschmann M. M. (2003) Partial melting experiments on a MORB-like pyroxenite between 2 and 3 GPa: constraints on the presence of pyroxenite in basalt source regions from solidus location and melting rate. *J. Geophys. Res.* 10.1029/2000JB000118.

Petter S. W. (1991) *Regional Geology of Africa*. Springer, Berlin, 722pp.

Pik R., Deniel C., Coulon C., Yirgu G., and Marty B. (1999) Isotopic and trace element signatures of Ethiopian flood basalts: evidence for plume–lithosphere interactions. *Geochim. Cosmochim. Acta,* **63**, 2263–2279.

Price R. C., Gray C. M., and Frey F. A. (1997) Strontium isotopic and trace element heterogeneity in the plains basalts of the Newer Volcanic Province, Victoria, Australia. *Geochim. Cosmochim. Acta* **61**, 171–192.

Puffer J. H. (2001) Contrasting high field strength element contents of continental flood basalts from plume versus reactivated-arc sources. *Geology* **29**, 675–678.

Reichow M. K., Saunders A. D., White R. S., Pringle M. S., Al'Mukhamedov A. I., Medvedev A. I., and Kirda N. P. (2002) 40Ar/39Ar dates from the West Siberian Basin: Siberian flood basalt province doubled. *Science* **296**, 1846–1849.

Reid M. R. and Graham D. W. (1996) Resolving lithospheric and sub-lithospheric contributions to helium isotope variations in basalts from the southwestern US. *Earth Planet. Sci. Lett.* **144**, 213–222.

Reid M. R. and Ramos R. (1996) Chemical dynamics of enriched mantle in the southwestern United States: thorium isotope evidence. *Earth Planet. Sci. Lett.* **138**, 239–254.

Reiners P. W., Nelson B. K., and Ghiorso M. S. (1995) Assimilation of felsic crust by basaltic magma: thermal limits and extents of crustal contamination of mantle-derived magmas. *Geology* **23**, 563–566.

Renne P. R. and Basu A. R. (1991) Rapid eruption of the Siberian Traps flood basalts at the Permo-Triassic boundary. *Science* **253**, 176–179.

Renne P. R., Ernesto M., Pacca I. G., Coe R. S., Glen J. M., Prevot M., and Perring M. (1992) The age of the Paraná flood volcanism, rifting of Gondwanaland, and the Jurassic–Cretaceous boundary. *Science* **246**, 975–979.

Renne P. R., Zichao Z., Richards M. A., Black M. T., and Basu A. R. (1995) Synchrony and causal relations between Permian–Triassic boundary crises and Siberian flood volcanism. *Science* **269**, 1413–1416.

Ringwood A. E., Kesson S. E., Hibberson W., and Ware N. (1992) Origin of kimberlites and related magmas. *Earth Planet. Sci. Lett.* **113**, 521–538.

Robert U., Foden J., and Varne R. (1992) The Dodecanese Province, SE Aegean: a model for tectonic control on potassic magmatism. *Lithos* **28**, 241–260.

Roeder P. L. and Emslie R. F. (1970) Olivine–liquid equilibrium. *Contrib. Mineral. Petrol.* **29**, 275–289.

Rogers N. W., James D., Kelley S. P., and de Mulder M. (1998) The generation of potassic lavas from the eastern Virunga Province, Rwanda. *J. Petrol.* **39**, 1223–1247.

Rollinson H. (1993) *Using Geochemical Data: Evaluation, Presentation, Interpretation*. Longman, Singapore.

Rudnick R., McDonough W. F., and O'Connell R. J. (1998) Thermal structure, thickness and composition of continental lithosphere. *Chem. Geol.* **145**, 395–411.

Rudnick R. L. (1992). Xenoliths-samples of the lower continental crust. In *Continental Lower Crust* (eds. D. M. Fountain, R. J. Arculus, and R. W. Kay), Developments in Geotectonics 23. Elsevier, Amsterdam, pp. 363–390.

Rudnick R. L., McDonough W. F., McCulloch M. T., and Taylor S. R. (1986) Lower crustal xenoliths from Queensland, Australia: evidence for deep crustal assimilation and fractionation of continental basalts. *Geochim. Cosmochim. Acta* **50**, 1099–1115.

Ryerson F. J. and Watson E. B. (1987) Rutile saturation in magmas: implications for Ti–Nb–Ta depletion in island-arc basalts. *Earth Planet. Sci. Lett.* **86**, 225–239.

Saunders A. D., Fitton J. G., Kerr A. C., Norry M. J., Kent R. W. (1997) The North Atlantic igneous province. In *Large Igneous Provinces* (eds. J. J. Mahoney and M. F. Coffin), Geophysical Monograph 100. American Geophysical Union, Washington, DC, pp. 45–94.

Sautter V., Haggerty S. E., and Field S. (1991) Ultra-deep (>300 km) ultramafic xenoliths: new petrologic evidence from the transition zone. *Science* **252**, 827–830.

Schaefer B. F., Turner S. P., Rogers N. W., Hawkesworth C. J., Williams H. M., Pearson D. G., and Nowell G. M. (2000) Re–Os isotope characteristics of postorogenic lavas: implications for the nature of young lithospheric mantle and its contribution to basaltic magmas. *Geology* **28**, 563–566.

Schmidt K. H., Botazzi P., Vannucci R., and Mengel K. (1999) Trace element partitioning between phlogopite, clinopyroxene and leucite lamproite melt. *Earth Planet. Sci. Lett.* **168**, 287–299.

Selverstone J., Pun A., and Condie K. C. (1999) Xenolithic evidence for Proterozoic crustal evolution beneath the Colorado Plateau. *Geol. Soc. Am. Bull.* **111**, 590–606.

Sharma M. (1997) Siberian Traps. In *Large Igneous Provinces* (eds. J. J. Mahoney and M. F. Coffin), Geophysical Monograph 100. American Geophysical Union, Washington, DC, pp. 273–295.

Shaw D. M. (1970) Trace element fractionation during anatexis. *Geochim. Cosmochim. Acta* **34**, 237–243.

Shirey S. B. and Walker R. J. (1998) The Re–Os isotope system in cosmochemistry and high-temperature geochemistry. *Ann. Rev. Earth Planet. Sci.* **26**, 423–500.

Sigurdsson H. (2000) Volcanic episodes and rates of volcanism. In *Encyclopedia of Volcanoes* (ed. H. Sigurdsson). Academic Press, San Diego, pp. 271–282.

Smith C. B. (1983) Pb, Sr and Nd isotopic evidence for sources of southern African Cretaceous kimberlites. *Nature* **304**, 51–54.

Spera F. J. (2000) Physical properties of magmas. In *Encyclopedia of Volcanoes* (ed. H. Sigurdsson). Academic Press, San Diego, pp. 171–190.

Stein M. and Hoffman A. W. (1994) Mantle plumes and episodic crustal growth. *Nature* **372**, 63–68.

Stewart J. H. (1998) Regional characteristics, tilt domains, and extensional history of the later Cenozoic Basin and Range Province, western North America. In *Accommodation Zones and Transfer Zones: The Regional Segmentation of the Basin and Range Province* (eds. J. E. Faulds and J. H. Stewart), Geological Society of America Special Paper 323. Geological Society of America, Boulder, CO, pp. 47–74.

Storey B. C., Mahoney J. J., and Saunders A. D. (1997) Cretaceous basalts in Madagascar and the transition between plume and continental lithosphere mantle sources. In *Large Igneous Provinces* (eds. J. J. Mahoney and M. F. Coffin), Geophysical Monograph 100. American Geophysical Union, Washington, DC, pp. 95–122.

Sun S. S. and McDonough W. F. (1989) Chemical and isotopic systematics of oceanic basalts: implications for mantle composition and processes. In *Magmatism in the Ocean Basins* (eds. A. D. Saunders and M. J. Norry). Geological Society, Oxford, pp. 313–345.

Tainton K. M. and McKenzie D. (1994) The generation of kimberlites, lamproites, and their source rocks. *J. Petrol.* **35**, 787–817.

Taylor H. P., Jr. (1968) The oxygen isotope geochemistry of igneous rocks. *Contrib. Mineral. Petrol.* **19**, 1–71.

Taylor W. R., Tompkins L. A., and Haggerty S. E. (1994) Comparative geochemistry of West African kimberlites: evidence for a micaceous kimberlite endmember of sublithospheric origin. *Geochim. Cosmochim. Acta* **58**, 4017–4037.

Thirlwall M. F., Upton B. G. J., and Jenkins C. (1994) Interaction between continental lithosphere and the Iceland Plume-Sr–Nd–Pb isotope geochemistry of Tertiary basalts, NE Greenland. *J. Petrol.* **35**, 839–879.

Thompson R. N. and Gibson S. A. (1994) Magmatic expression of lithospheric thinning across continental rifts. *Tectonophysics* **233**, 41–68.

Turner S., Arnaud N., Liu J., Rogers N., Hawkesworth C., Harris N., Kelley S., Van Calsteren P., and Deng W. (1996a) Post-collision, shoshonitic volcanism on the Tibetan lateau: implications for convective thinning of the lithosphere and the source of ocean island basalts. *J. Petrol.* **37**, 45–71.

Turner S., Hawkesworth C. J., Gallagher K., Stewart K., Peate D. W., and Mantovani M. (1996b) Mantle plumes, flood basalts, and thermal models for melt generation beneath continents: assessment of a conductive heating model and application to the Parana′. *J. Geophys. Res.* **101**, 11503–11518.

Valley J. W. (1986). Stable isotope geochemistry of metamorphic rocks. In *Stable Isotopes in High Temperature Geological Processes* (ed. P. H. Ribbe). *Rev. Mineral.*, Mineralogical Society of America, Chelsea, MI, vol. 16, pp. 445–490.

Walker R. J., Carlson R. W., Shirey S. B., and Boyd F. R. (1989) Os, Sr, Nd, and Pb isotope systematics of southern African peridotite xenoliths: implications for the chemical evolution of subcontinental mantle. *Geochim. Cosmochim. Acta* **53**, 1583–1595.

Wang K., Plank T., Walker J. D., and Smith E. I. (2002) A mantle melting profile across the Basin and Range SW USA. *J. Geophys. Res.* **107**, doi:10.1029/2001JB000209.

Wedepohl K. H. (2000) The composition and formation of Miocene tholeiites in the Central European Cenozoic plume volcanism (CECV). *Contrib. Mineral. Petrol.* **140**, 180–189.

Wedepohl K. H. and Baumann A. (1999) Central European Cenozoic plume volcanism with OIB characteristics and indications of a lower mantle source. *Contrib. Mineral. Petrol.* **136**, 225–239.

Wernicke B. P., Axen G. T., and Snow J. S. (1988) Basin and range extensional tectonics at the latitude of Las Vegas, Nevada. *Geol. Soc. Am. Bull.* **100**, 1738–1757.

White R. S. (1988) The Earth's crust and lithosphere. *J. Petrol.* (Spec. Lithosphere Issue), 1–10.

Wilshire H. W., McGuire A. V., Noller J. S., and Turrin B. D. (1991) Petrology of lower crustal and upper mantle xenoliths from the Cima Volcanic Field, California. *J. Petrol.* **32**, 169–200.

Wilson M. and Patterson R. (2001) Intraplate magmatism related to short-wavelength convective instabilities in the upper mantle: evidence from the Tertiary–Quaternary volcanic province of western and central Europe. In *Mantle Plumes: Their Identification through Time* (eds. R. E. Ernst and K. L. Buchan), Geological Society of American Special Paper 352. Geological Society of America, Boulder, CO, pp. 37–58.

Wilson M., Tankut A., and Gulec N. (1997) Tertiary volcanism of the Galatia province, north-west Central Anatolia, Turkey. *Lithos* **42**, 105–122.

Winter J. D. (2001) *An Introduction to Igneous and Metamorphic Petrology*. NJ: Prentice Hall, Upper Saddle River.

Wooden J. L., Czamanske G. K., Fedorenko V. A., Arndt N. T., Chauvel C., Bouse R. M., King B. W., Knight R. J., and Siems D. F. (1993) Isotopic and trace-element constraints on mantle and crustal contributions to Siberian continental flood basalts, Noril'sk area, Siberia. *Geochim. Cosmochim. Acta* **57**, 3677–3704.

Woolley A. R., Bergman S. C., Edgar A. D., Le Bas M. J., Mitchell R. G., Rock N. M. S., and Scott-Smith B. H. (1996) Classification of lamprophyres, lamproites, kimberlites, and the kalsilitic, melitic, and leucitic rocks. *Can. Mineral.* **34**, 175–186.

Wyllie P. J. and Huang W. L. (1976) Carbonation and melting reactions in the system $CaO–MgO–SiO_2–CO_2$ at mantle pressures with geophysical and petrologic applications. *Contrib. Mineral. Petrol.* **54**, 79–107.

Zhang M. and O'Reilly S. Y. (1997) Multiple sources for basaltic rocks from Dubbo, eastern Australia: geochemical evidence for plume–lithosphere interaction. *Chem. Geol.* **136**, 33–54.

Zhang M., Stephenson P. J., O'Reilly S. Y., McCulloch M. T., and Norman M. (2001) Petrogenesis and geodynamic implications of Late Cenozoic basalts in North Queensland, Australia: trace element and Sr–Nd–Pb isotope evidence. *J. Petrol.* **42**, 685–719.

Zhang M., Suddaby P., Thompson R. N., Thirlwall M. F., and Menzies M. A. (1995) Potassic volcanic rocks in NE China: geochemical constraints on mantle source and magma genesis. *J. Petrol.* **36**, 1275–1303.

Zhou M. F., Malpas J., Song S. H., Robinson P. T., Sun M., Kennedy A. K., Lesher C. M., and Keays R. R. (2002) A temporal link between the Emeishan large igneous province (SW China) and the end-Guadalupian mass extinction. *Earth Planet. Sci. Lett.* **196**, 113–122.

Zindler A. and Hart S. (1986) Chemical geodynamics. *Ann. Rev. Earth Planet. Sci.* **14**, 493–571.

Zou H. and Reid M. R. (2001) Quantitative modeling of trace element fractionation during incongruent dynamic melting. *Geochim. Cosmochim. Acta* **65**, 153–162.

Zou H., Zindler A., Xu X., and Qi Q. (2000) Major, trace element, and Nd, Sr and Pb isotope studies of Cenozoic basalts in SE China: mantle sources, regional variations, and tectonic significance. *Chem. Geol.* **171**, 33–47.

© 2007, Elsevier Ltd. All rights reserved.
No part of this publication may be reproduced, stored in a retrieval system or transmitted in any form or by any means, electronic, mechanical, photocopying, recording or otherwise, without prior written permission of the Publisher.

Treatise On Geochemistry
ISBN (set): 0-08-043751-6
pp. 1–39